Journal of Statistical Physics, Vol. 116, No. 5/6, September 2004 (© 2004)

Metastable States, Transitions, Basins and Borders at Finite Temperatures

Sorin Tănase-Nicola[1] **and Jorge Kurchan**[1]

Received November 25, 2003; accepted January 3, 2004

Langevin/Fokker-Planck processes can be immersed in a larger frame by adding fictitious fermion variables. The (super) symmetry of this larger structure has been used to derive Morse theory in an elegant way. The original physical diffusive motion is retained in the zero-fermion subspace. Here we study the subspaces with non-zero fermion number which yield deep information, as well as new computational strategies, for barriers, reaction paths, and unstable states – even in non-zero temperature situations and when the barriers are of entropic or collective nature, as in the thermodynamic limit. The presentation is self-contained.

KEY WORDS: Reaction paths; Metastability; Stochastic methods; Kramers' problem; Morse theory.

1. INTRODUCTION

Many systems have a dynamics with processes which take place on distinct timescales. The most familiar example is the diffusion in a many-valley energy $E(\boldsymbol{x})$ landscape at low temperatures:

$$\dot{x}_i = -\frac{\partial E}{\partial x_i} + \sqrt{2T}\,\eta_i, \tag{1}$$

which consists of rapid gradient descents into local minima, and slow 'activated' transitions between minima induced by the thermal noise η_i (Gaussian independent white noises of unit variance). The relevant parameter is the inverse temperature $\beta = 1/T$: the larger β the more pronounced

[1]PMMH UMR 7636 CNRS-ESPCI, 10, Rue Vauquelin, 75231 Paris CEDEX 05, France; e-mail: kurchan@1pt.ens.fr

0022-4715/04/0900-1201/0

the gap between fast intra-valley relaxations and slow activation processes $\ln(t_{slow}) \sim \beta \Delta E$.[1] Another example is that of cooperative systems at finite temperature. Consider for example a d-dimensional ferromagnet in a magnetic field h pointing upward: the state with negative magnetization becomes unstable, its decay taking a time $\ln(t_{slow}) \propto h^{-(d-1)}$, the parameter controlling the timescale separation is the inverse of the field. In the absence of field, the slow relaxation takes a time $\ln(t_{slow}) \propto L^{d-1}$, and the control parameter is the size L.[2] From a conceptual point of view, it is important in these situations to characterize the relevant structures: metastable states and their basins of attraction, the reaction paths joining them, and the timescales involved. On the other hand, in order to efficiently model realistic situations, one needs to be able to treat the rare 'activated' passages in a specific way.

Quite generally, a separation between timescales implies the existence of metastable states, defined as probability distributions corresponding to situations in which everything fast has happened and everything slow has not taken place. If there are more than two timescales, for example $t_{fast} \ll t_{interm} \ll t_{slow}$ one has metastable states at t_{interm}, and a different set of metastable states at t_{slow}, the latter resulting from the fusion or the decay of states defined for t_{interm}. Given how natural the concept of metastability is, it may come as a surprise that only recently has a construction of metastable states based on the stochastic dynamics been fully established.[3]

The idea is simple: the probability associated with Eq. (1) evolves through:[14]

$$\frac{dP(\boldsymbol{x},t)}{dt} = -H_{FP}\, P(\boldsymbol{x},t),$$
$$H_{FP} = -\sum_{i=1}^{N} \frac{\partial}{\partial x_i}\left(T\frac{\partial}{\partial x_i} + E_{,i}\right), \tag{2}$$

(from here onward we denote derivatives as $A_{,i} \equiv \frac{\partial A}{\partial x_i}$ and $A_{,ij} \equiv \frac{\partial^2 A}{\partial x_i \partial x_j}$) where H_{FP} is the Fokker-Planck operator and N the number of dimensions of the space. It turns out[3] that if there is a separation of timescales $t_{fast} \ll t_{slow}$ in the system, the spectrum of H_{FP} has a gap: there are (say) K eigenvalues of the order of t_{slow}^{-1} and all other eigenvalues are at least of the order of t_{fast}^{-1}. Furthermore, one can show that, in the limit of large timescale separation, irrespective of its origin, one can construct exactly K probability distributions corresponding to distinct metastable states by linear combinations of the K eigenstates 'below the gap'. The low temperature example is particularly clear: in that case these K distributions are Gaussians of width $\sqrt{T}$ sitting at each of the K local minima.

In a situation with metastability, it becomes interesting and in practice necessary to evaluate the time of decay, as well as the spatial probability distribution of the escape current (i.e. the reaction paths). This may involve identifying the barrier or 'bottleneck' responsible for the slowness of decay. In the low temperature example, the reaction paths are simply gradient lines connecting two energy minima through a saddle with one unstable direction (of index one). The bottlenecks are these saddle-points, and there is a considerable variety of methods for their location in high dimensional space.[15]

Now, there is a construction that naturally incorporates saddle points, and that has been successfully used to derive the relations between the numbers of saddle points of a function (the energy here) and the topological properties of the manifold on which it is defined. These relations are the so-called Morse inequalities,[16] and have been rederived in an elegant and elementary way by Witten.[17] The construction is a 'completion' of the diffusive problem as follows. First express the Fokker-Planck operator in a basis in which it is manifestly Hermitian:[14]

$$H^h_{FP} = e^{\beta E/2} H_{FP} e^{-\beta E/2} = \frac{1}{T} \sum_{i=1}^{N} \left[-T^2 \frac{\partial^2}{\partial x_i^2} + \frac{1}{4} E_{,i}^2 - \frac{T}{2} E_{,ii} \right]. \tag{3}$$

Second, 'complicate' the operator and the space by introducing N fermions $a_i^\dagger$, a_i, with $i = 1, \ldots, N$, and:

$$\begin{aligned} H^h &= H^h_{FP} + \sum_{ij=1}^{N} E_{,ij} a_j^\dagger a_i \\ &= \frac{1}{T} \sum_{i}^{N} \left[-T^2 \frac{\partial^2}{\partial x_i^2} + \frac{1}{4} E_{,i}^2 - \frac{T}{2} E_{,ii} \right] + \sum_{ij=1}^{N} E_{,ij} a_j^\dagger a_i = (H^h)^\dagger. \end{aligned} \tag{4}$$

Within zero-fermion subspace, H^h is just the Hermitian form of the Fokker-Planck operator, and, as we have remarked, for low temperatures its eigenstates 'below the gap' are related to local minima.

The wave-functions with one or more fermions are so far a spurious addition. Their interest stems from the fact that one can show that there is a gap in all the spectra associated with any fermion number, and the states 'below the gap' having one fermion are for low temperatures peaked on saddles with one unstable direction, those having two fermions on saddles with two unstable directions, and in general those with p fermions on saddles of index p. Using this fact and the symmetries of H^h, it is then easy to derive Morse inequalities[17] – we shall review this in Section 3.

The basis that makes H_{FP} Hermitian as in Eq. (3) (we shall in what follow refer to it as the 'Hermitian basis') offers the direct way to get to Morse theory, and is the one most often used in the field theory literature. Here, we are mainly interested in the diffusive interpretation, at least of the original zero-fermion subspace, and for this we must go back to the original basis.[18] The change from the Hermitian to the original basis is made by a multiplication by $e^{\beta E/2}$, and is quite tricky since it is exponentially large in the relevant parameter — β if we are interested in the low temperature limit, or the system size for macroscopic systems. Because of this reason, one has to be very careful because negligible, large deviations in one basis become of $O(1)$ in the other. Indeed, the strategy we shall follow in this paper is to rederive the limit wave functions in each basis from scratch.

A first question we may ask is how do the eigenstates 'below the gap' with fermion number larger than zero look, for low temperatures, in the original basis in which

$$H = H_{FP} + \sum_{ij=1}^{N} E_{,ij} a_j^\dagger a_i = e^{-\beta E/2} H^h e^{\beta E/2}. \tag{5}$$

The outcome, as we shall see, is a pleasant surprise: for example one fermion (right) eigenstates 'below the gap' are concentrated not on the saddle, but along a narrow (width $\sim \sqrt{T}$) tube following the gradient line joining minima and passing through the saddle – the reaction path. Higher fermion number subspaces (and *left* eigenstates) also encode interesting information.

The construction yielding Morse theory relies on the low-temperature limit, in which functions peak on the appropriate structures. Low temperatures are just one instance of evolution with widely separated scales. One is naturally led to ask what happens with the construction we have described in the presence of a timescale separation generated by some other (collective, entropic...) mechanism. Again, the answer is pleasant: for example the one fermion eigenstates 'below the gap' of (5) yield the reaction current distributions between metastable states (the latter defined dynamically as outlined after Eq. (2)). This generalization will give us practical strategies for the evaluation of reaction paths, valid whenever there is timescale separation. From a more abstract point of view, it will yield a precise definition of 'free energy barrier' in a natural way, without having to rely on mean-field or any other approximation.

Let us write, for a generic wavefunction $|\psi\rangle$, an evolution equation:

$$\frac{d|\psi\rangle}{dt} = -H\,|\psi\rangle. \tag{6}$$

Specializing ψ to zero fermions we recover the Fokker-Planck equation (2). Consider now Eq. (6) but within the one-fermion subspace, in which functions are of the form $|\xi^R\rangle = \int d^N x \sum_{c=1}^N R_c(\boldsymbol{x})|\boldsymbol{x}\rangle a_c^\dagger|-\rangle$, with $|\boldsymbol{x}\rangle$ the basis in space and $|-\rangle$ the fermion vacuum. It amounts to an evolution for a *vector* function $\boldsymbol{R}(\boldsymbol{x},t) = (R_1(\boldsymbol{x},t), \ldots, R_N(\boldsymbol{x},t))$:

$$\frac{dR_c(\boldsymbol{x},t)}{dt} = -H_{FP}\, R_c(\boldsymbol{x},t) - \sum_{b=1}^{N} \frac{\partial^2 E}{\partial x_c \partial x_b} R_b(\boldsymbol{x},t). \tag{7}$$

Equation (7) is one of the main instruments of this paper. It evolves a vector field $\boldsymbol{R}(\boldsymbol{x},t)$ so that it rapidly becomes a linear combination of one fermion states 'below the gap'.

In a system with metastable states, starting from an initial condition, the probability distribution $P(\boldsymbol{x},t)$ evolves rapidly to a quasi-stationary distribution corresponding to quasi-equilibrium within one or more metastable states. At longer timescales, $P(\boldsymbol{x},t)$ will be gradually concentrated on new, more stable metastable states. If we choose the initial condition to be close to a state, we get a quick thermalization within such a state. What we have been discussing up to now suggests that Eq. (7) does for reaction currents what the Fokker-Planck equation does for states: depending on the initial conditions, $\boldsymbol{R}(\boldsymbol{x},t)$ tends rapidly to a reaction current between metastable states, which, in the particular case of very low temperatures, is a single reaction path. As time passes, other new current distributions start contributing to $\boldsymbol{R}(\boldsymbol{x},t)$.

The main point is that while escape from a state takes by assumption long times for the probability distribution $P(\boldsymbol{x},t)$, convergence to a reaction current is for $\boldsymbol{R}(\boldsymbol{x},t)$ immediate (or more precisely, of the same order of the time it takes for $P(\boldsymbol{x},t)$ to stabilize in the closest state). Now, a whole set of practical methods, such as simulated annealing and transition path sampling, can be seen as ways of implementing the Fokker-Planck equation — the former in a diffusive and the latter in a functional way. The same can be done with Eq. (7): we shall give in this paper a diffusion equation which is to Eq. (7) what the Langevin process is to Eq. (2), and a path-sampling procedure based on Eq. (7) which has the peculiarity that the paths pile up on the barriers.

To conclude this rather technical introduction, let us summarize what we do in this paper. We first (Section 2) introduce the supersymmetric construction in detail, stressing in particular the relation between the original Fokker-Planck basis and the Hermitian basis. As a first example, in Section 3 we rederive Morse theory for the case of smooth potentials in a simply connected space.

In Section 4, after briefly reviewing the dynamic definition of metastable states, we analyze in detail the structure of the one fermion subspace, showing that it contains the reaction paths and also 'loops': reactions leading from a state to itself. Although for clarity we always keep the low-temperature case in mind, the developments are valid whatever the origin of the timescale separation.

In Section 5 we summarize the structure in all fermion subspaces. For the low-temperature case we discuss the form of all eigenstates 'below the gap'. The derivation of these results can be made in an explicit way using a diffusive dynamics we introduce in Section 6, which plays for the higher fermion number subspaces the role that Langevin equation plays for the zero-fermion Fokker-Planck evolution.

In Section 7 we construct a path-sampling process to locate reaction paths, in which the trajectories are weighed with the usual Langevin action plus a Lyapunov exponent associated to each trajectory.

2. SUPERSYSMETRIC QUANTUM MECHANICS AND FOKKER-PLANCK EQUATION

We assume that $E(\boldsymbol{x})$ is two times differentiable and that the Gibbs measure exists:

$$\int_{R^N} d^N x\, e^{-\beta E} < \infty. \tag{8}$$

The dynamics of the system is given by the Langevin equation (1). The probability distribution will evolve according to the Fokker Planck equation (2), which can be seen as a continuity equation for the current:[14]

$$J_i(\boldsymbol{x}, t) \equiv \left(T \frac{\partial}{\partial x_i} + E_{,i} \right) P(\boldsymbol{x}, t). \tag{9}$$

We introduce at this point N fermion creation and annihilation operators $a_i^\dagger$ and a_i, with anticommutation relations $[a_i, a_j^\dagger]_+ = \delta_{ij}$; the fermion number operator is $N_f = \sum_{i=1}^N a_i^\dagger a_i$. We denote states in the coordinate space as $|\psi\rangle$ and $\psi(\boldsymbol{x}) \equiv \langle \boldsymbol{x}|\psi\rangle$, using the Dirac bra-ket notation of Quantum Mechanics; the zero-fermion state is $|-\rangle$, and we denote states in the product space (coordinate $\otimes$ fermions) with boldface. We say that $|\boldsymbol{\psi}\rangle$ has n fermions if:

$$N_f |\boldsymbol{\psi}\rangle = n |\boldsymbol{\psi}\rangle. \tag{10}$$

We define the 'charges'

$$\bar{Q} = -\mathrm{i}\sum_{i=1}^{N}(T\frac{\partial}{\partial x_i} + E_{,i})a_i^\dagger; \quad Q = -\mathrm{i}T\sum_{i=1}^{N}\frac{\partial}{\partial x_i}a_i, \tag{11}$$

which satisfy:

$$\bar{Q}^2 = Q^2 = 0. \tag{12}$$

We can write the operator

$$H = \frac{1}{T}(\bar{Q} + Q)^2 = \frac{1}{T}[\bar{Q}, Q]_+ = H_{FP} + \sum_{ij=1}^{N} E_{,ij}a_j^\dagger a_i, \tag{13}$$

where

$$[H, Q] = [H, \bar{Q}] = 0. \tag{14}$$

H commutes with the fermion number operator N_f, so that eigenstates are classified according to their fermion number. Within the zero-fermion space, H is the original Fokker-Planck operator. These relations are true only for the Fokker-Planck equation with the drift forces at least locally a gradient. Q and $\bar{Q}$ commute with H and transform states with an even number of fermions (bosonic states) into those with an odd number of fermions (fermionic states) and vice-versa, hence the name 'supersymmetry'. What we have done up to now can be seen as completing the square, and making symmetries underlying the Fokker-Planck equation *with gradient forces* explicit.

One can now make a change of basis such that the charges become Hermitian conjugates of one another:

$$\begin{aligned} Q^h &= e^{\beta E/2}Qe^{-\beta E/2} = -\mathrm{i}\sum_{i=1}^{N}(T\frac{\partial}{\partial x_i} - \frac{1}{2}E_{,i})a_i, \\ \bar{Q}^h &= e^{\beta E/2}\bar{Q}e^{-\beta E/2} = -\mathrm{i}\sum_{i=1}^{N}(T\frac{\partial}{\partial x_i} + \frac{1}{2}E_{,i})a_i^\dagger = (Q^h)^\dagger. \end{aligned} \tag{15}$$

In the new basis we have the Hermitian equivalent of Eq. (13):

$$H^h = \frac{1}{T}[\bar{Q}^h, Q^h]_+ = \frac{1}{T}(\bar{Q}^h + Q^h)^2 = H^h_{FP} + \sum_{ij=1}^{N} E_{,ij} a_j^\dagger a_i$$
$$= \frac{1}{T}\sum_{i=1}^{N}\left[-T^2\frac{\partial^2}{\partial x_i^2} + \frac{1}{4}E_{,i}^2 - \frac{T}{2}E_{,ii}\right] + \sum_{ij=1}^{N} E_{,ij} a_j^\dagger a_i = (H^h)^\dagger. \quad (16)$$

H^h_{FP} has now the standard form of a Schrödinger operator (acting in imaginary time) with T playing the role of $\hbar$. On the other hand H^h is the standard Hamiltonian of Supersymmetric Quantum Mechanics.[24]

As the original operators H_{FP} and H are not hermitian we will have two different eigenvalue equations, one for the right eigenstates ($|\boldsymbol{\psi}^{\boldsymbol{R}}\rangle$) and one for the left eigenstate ($\langle\boldsymbol{\psi}^{\boldsymbol{L}}|$)

$$H|\boldsymbol{\psi}^{\boldsymbol{R}}\rangle = \lambda|\boldsymbol{\psi}^{\boldsymbol{R}}\rangle;\ \langle\boldsymbol{\psi}^{\boldsymbol{L}}|H = \lambda\langle\boldsymbol{\psi}^{\boldsymbol{L}}|, \quad (17)$$

while in the Hermitian basis there will be only one equation

$$H^h|\boldsymbol{\psi}^{\boldsymbol{h}}\rangle = \lambda|\boldsymbol{\psi}^{\boldsymbol{h}}\rangle. \quad (18)$$

The three states are related by

$$|\boldsymbol{\psi}^{\boldsymbol{R}}\rangle = e^{-\beta E/2}|\boldsymbol{\psi}^{\boldsymbol{h}}\rangle;\ |\boldsymbol{\psi}^{\boldsymbol{L}}\rangle = e^{\beta E/2}|\boldsymbol{\psi}^{\boldsymbol{h}}\rangle. \quad (19)$$

It is clear that H and H^h have the same spectrum. Furthermore, the relation:

$$H^\dagger = -\sum_{i=1}^{N}\frac{\partial}{\partial x_i}\left[T\frac{\partial}{\partial x_i} - E_{,i}\right] - \sum_{ij=1}^{N} E_{,ij} a_j a_i^\dagger, \quad (20)$$

implies that a left k-fermion eigenstate of H is an $N-k$ right eigenstate of the problem with the inverted potential $-E$.

From Eqs. (13) and (4), we see that H and H^h have non-negative eigenvalues. By construction, there is at least one eigenstate $|\boldsymbol{\psi}^{\boldsymbol{0h}}\rangle$ corresponding to the eigenvalue $\lambda = 0$ (the smallest possible):

$$\begin{aligned} |\boldsymbol{\psi}^{\boldsymbol{0h}}\rangle &\propto e^{-\beta E/2} \otimes |-\rangle, \\ |\boldsymbol{\psi}^{\boldsymbol{0R}}\rangle &\propto e^{-\beta E} \otimes |-\rangle, \\ |\boldsymbol{\psi}^{\boldsymbol{0L}}\rangle &\propto \text{constant } |-\rangle. \end{aligned} \quad (21)$$

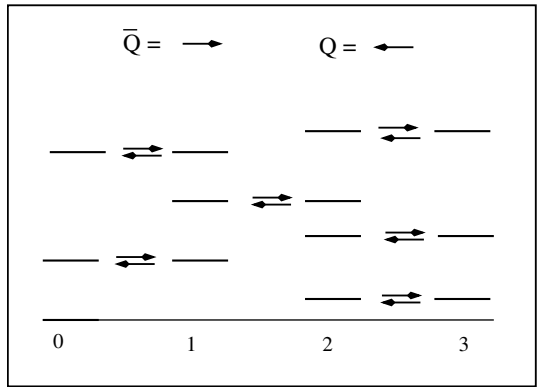

Fig. 1. The pairing of the energy levels for a generic spectrum. Each eigenstate of positive energy has a supersymmetric partner. The number of fermions is written below each corresponding column. The only unpaired state is the zero-energy one.

In order for $|\psi^{0h}\rangle$ to be normalizable we need the convergence of the integral (8).

The left and right eigenstates (22) have zero fermions and, thus, they belong also to the spectrum of H_{FP}. Clearly, both Q and $\bar{Q}$ annihilate $|\psi^{0R}\rangle$. It is easy to show (see Appendix A) that this is necessary for any zero eigenvector, and indeed Eq. (22) are the only ones with this property *if the space has no holes*.

In general applying Q to any eigenstate $|\psi^R\rangle$ we get either a degenerate eigenstate with one less fermion or zero. Similarly, applying $\bar{Q}$ we get either a degenerate eigenstate with one more fermion or zero. Each non-zero energy eigenstate $|\psi^R\rangle$, annihilated by Q, can be written as $|\psi^R\rangle = Q|\chi^R\rangle$, and the same holds for $\bar{Q}$. Indeed, from the eigenvalue equation

$$H|\psi^R\rangle = \frac{1}{T}(\bar{Q}Q + Q\bar{Q})|\psi^R\rangle = \frac{1}{T}Q\bar{Q}|\psi^R\rangle = \lambda|\psi^R\rangle, \tag{22}$$

one can infer that

$$|\chi^R\rangle = \frac{1}{T\lambda}\bar{Q}|\psi^R\rangle, \tag{23}$$

satisfies $Q|\chi^R\rangle = |\psi^R\rangle$.

In conclusion, each non-zero energy eigenstate with k fermions, will have one and only one supersymmetric partner with either $k-1$ or $k+1$ fermions. In a space with no holes the only eigenstate with zero energy has

zero fermions and is the Gibbs measure (See Appendix A). The spectrum is organized as in Fig. 1.

3. MORSE THEORY

In the low temperature limit, the organization of the spectrum of H^h allows to derive relations concerning the critical points (saddles) of the energy surface, defined as those points for which

$$|\nabla E|^2 = \sum_{i=1}^{N} E_{,i}^2 = 0. \tag{24}$$

Let us study the *semiclassical* low-T spectrum. At the lowest order in T, the potential appearing in the Schrödinger operator (4)

$$W = \frac{1}{T} \sum_{i=1}^{N} \frac{1}{4} E_{,i}^2, \tag{25}$$

is very large except at the critical points of E; so the eigenstates of H^h with low-lying eigenvalues are concentrated around the those critical points.

Let us assume that the critical points are isolated and the Hessian $E_{,ij}$ has non zero eigenvalues. Then, as usual, the semiclassical development starts with a harmonic approximation around each minimum of W. Consider one of these minima, where the Hessian has eigenvalues $A_1, \ldots, A_N$. We can develop E in the local coordinates, and going to the basis in which the Hessian $E_{,ij}$ is diagonal, we have that, locally:

$$E(\boldsymbol{x}') \sim E_0 + \frac{A_i}{2} x_i'^2. \tag{26}$$

We can develop H at the first order in T as

$$\frac{T}{2} H' = \sum_{i=1}^{N} \left\{ -\frac{T^2}{2} \frac{\partial^2}{\partial x_i'^2} + \frac{1}{2} \left(\frac{A_i}{2} \right)^2 x_i'^2 - \frac{T}{4} A_i + \frac{T}{2} A_i a_i'^{\dagger} a_i' \right\}. \tag{27}$$

We recognize the Hamiltonian of N independent oscillators plus N independent fermion terms. Along each direction i on the right hand side, we have a harmonic oscillator with *positive* frequency $|A_i|$, plus terms which give $-A_i/2$ if there is no fermion and $+A_i/2$ if there is a fermion along

the direction i. Hence, each fermion term will exactly cancel the zero-point energy of each oscillator, provided we have zero fermions if $A_i > 0$ and one fermion if $A_i < 0$. All in all, we see that we get zero to this order if and only if we have exactly as many fermions as unstable directions in the particular critical point.[25]

The next higher eigenvalues λ are given by, to leading order:

$$\lambda \sim \frac{1}{2} \sum_{i=1}^{N} [(2N_i + 1)|A_i| - A_i + 2A_i n_i)], \tag{28}$$

with $N_i = 0, 1, 2, \ldots$ and n_i is the number of fermions ($n_i = 0, 1$) for each direction. The spatial part of the eigenstates are Gaussians times polynomials, thus having widths of order $\sqrt{\frac{T}{A_i}}$ in the i^{th} direction so the approximation is consistent at low T.

Let us call saddle of index p a critical point whose Hessian has p negative eigenvalues, and M_p the number of these. For example the minima are saddles of order 0 while the saddles of order N are maxima. From the above considerations it follows that around each saddle of index p there there is one and only one state with zero energy as $T \to 0$, and this state has p fermions. This means that the Hamiltonian (4) has, to this order, M_p p-fermion eigenstates with a zero energy. As a consequence, there is a gap in the eigenvalues of each fermion sector, and the spectrum looks like Fig. 2.[26]

Recalling that any non-zero energy eigenstate with p fermions has a degenerate partner with either $p-1$ or $p+1$ fermions (cfr. Section 1), one can read from Fig. 2 the relations:

$$\begin{aligned} M_0 &= 1 + K_1, \\ M_1 &= K_1 + K_2, \\ M_2 &= K_2 + K_3, \\ &\vdots \\ M_N &= K_N, \end{aligned} \tag{29}$$

where K_p is the number of states of p fermions which have partners with $p-1$ fermions. The positivity of the K's ($K_i \geqslant 0 \forall i$) are the strong Morse inequalities.

We have used the condition that E is defined in a space without holes. As we have seen (see Appendix A) this implies that there is only one eigenstate of zero energy and it has zero fermions. If the space has a more com-

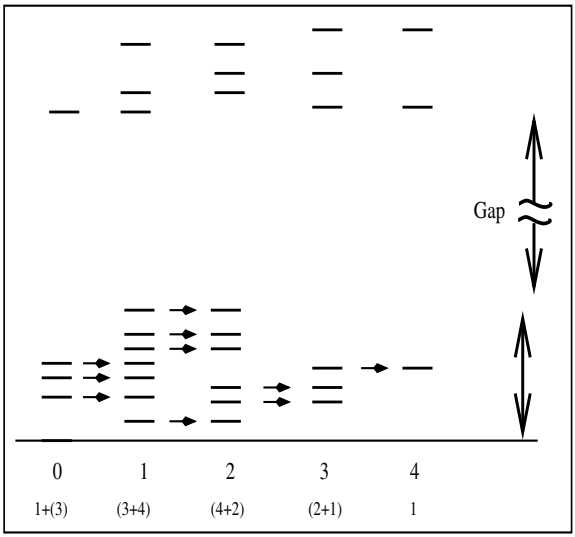

Fig. 2. Morse Theory. The arrows indicate the action of $\bar{Q}$. The gap in the spectrum means that the ratio of the lowest eigenvalue above the gap to the highest below the gap becomes infinite at small T. The numbers between brackets indicate the number of states below the gap of each fermion number decomposed as in Eq. (30); the Morse inequalities are evident from the picture.

plicated topology, there will be several zero-energy eigenstates not paired by the supersymmetric charges, and the Morse inequalities become slightly more complicated (see Appendix B).

4. STATES AND TRANSITION CURRENTS

4.1. A Simple Case

In the previous section we have given the form of the spectrum, at least to leading order, and the corresponding wave functions of every fermion number – the latter in the Hermitian basis. It may seem that going to the original basis is trivial since it is simply a matter of multiplying those approximate wave functions by $e^{\beta E/2}$. As mentioned above, this is rather tricky, since the factor $e^{\beta E/2}$ will resurrect large deviations which we have neglected.

Let us first study the simple case of a double well at low temperatures. We consider a probability distribution P evolving under the action of the Fokker-Plank Hamiltonian (2) corresponding to an energy as in Fig. 3. This distribution can be decomposed on the eigenstates of the Fokker-Planck Hamiltonian (ie. the zero-fermion eigenstates of the

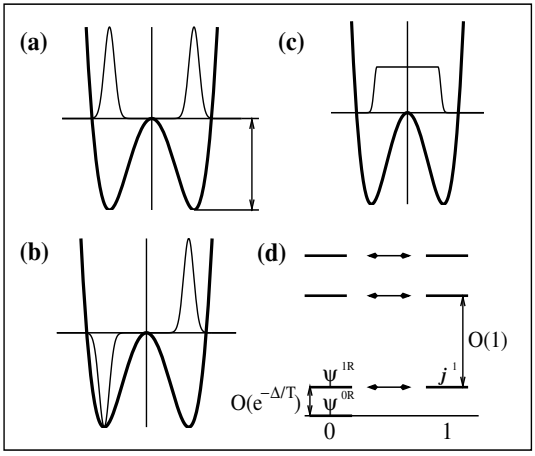

Fig. 3. The potential and different eigenstates along the reaction coordinate; (a) is the equilibrium density (ψ^{0R}), (b) the first eigenstate - the most stable (ψ^{1R}), (c) is the current density (j^1) from the first eigenstate and (d) the spectrum with the gap and the two fermionic sectors.

Hamiltonian (13))

$$P(x,t)=\sum_{\alpha=0}^{\infty} c_\alpha \psi^{\alpha R} e^{-\lambda_\alpha t}, \tag{30}$$

where $\psi^{0R}=e^{-\beta E}$ while $\lambda_0=0$. The constants c_α are obtained from the initial probability distribution as: $c_\alpha=\int d^N x\, \psi^{\alpha L}(x) P(x,0)$.

In the low temperature limit there are two metastable states each concentrated around one of the minima. Barrier penetration leads to the Gibbs measure, the symmetric combination of those states. In fact the spectrum of the Fokker-Planck Hamiltonian will contain one zero eigenvalue $\lambda_0=0$ (the Gibbs measure), one small $\lambda_1 \sim O(e^{-\Delta/T})$ eigenvalue and the rest of them much larger ($O(1)$). The two pure states, localized on the right and on the left are $\propto \psi^{0R}(x) \pm \psi^{1R}(x)$, respectively. If we are interested in the dynamics of the passage between the two wells we have to consider times such that the fast relaxation within each well has already taken place. At such times, larger than $t_1 \sim \frac{1}{\lambda_2} log(\frac{c_2}{c_1})$, we are left only with a distribution

$$P(x, t \gg t_1) \simeq c_0 \psi^{0R} + c_1 \psi^{1R} e^{-\lambda_1 t}, \tag{31}$$

i.e. a combination of states localized to the right and to the left, dependent upon the initial condition and time.

The current at any time is given by:

$$j(x,t) = \left(T\frac{\partial}{\partial x} + \frac{\partial E}{\partial x}\right) P(x,t) = \sum_{\alpha=1}^{\infty} c_\alpha e^{-\lambda_\alpha t} \left(T\frac{\partial}{\partial x} + \frac{\partial E}{\partial x}\right) \psi^{\alpha R}, \quad (32)$$

and its divergence reads:

$$\frac{\partial j}{\partial x} = \frac{\partial}{\partial x}\left(T\frac{\partial}{\partial x} + \frac{\partial E}{\partial x}\right) P(x,t) = -\sum_{\alpha=1}^{\infty} \lambda_\alpha c_\alpha e^{-\lambda_\alpha t} \psi^{\alpha R}. \quad (33)$$

We can split the contribution of each term as:

$$I^\alpha \equiv \lambda_\alpha c_\alpha e^{-\lambda_\alpha t} \psi^{\alpha R}. \quad (34)$$

All the contributions except I^1 eventually vanish, for example:

$$\frac{I^2}{I^1} \sim \frac{c_2\lambda_2 e^{-\lambda_2 t}}{c_1\lambda_1 e^{-\lambda_1 t}} \ll 1, \quad (35)$$

at times such that $t \gg t_2 \sim \frac{1}{\lambda_2} log(\frac{c_2\lambda_2}{c_1\lambda_1})$.[28]

Equation (33) now implies that the late-time regime current $j(x, t \gg t_2)$ is:

$$j(x, t \gg t_2) \simeq c_1\lambda_1 e^{-\lambda_1 t} \int_x^\infty dx\, \psi^{1R}(x), \quad (36)$$

and can be expressed using the one-fermion right eigenstate 'below the gap':

$$|\boldsymbol{\xi}^{\mathbf{1R}}\rangle = \bar{Q}|\boldsymbol{\psi}^{\mathbf{1R}}\rangle = \int dx\, \xi^{1R}(x)\, a^\dagger |x\rangle \otimes |-\rangle. \quad (37)$$

as $j(x, t \gg t_2) = ic_1 e^{-\lambda_1 t} \xi^{1R}(x)$.

In Fig. 3 we summarize the situation. Note that although the state $|\boldsymbol{\xi}^{\mathbf{1h}}\rangle$ is sitting on the saddle (as we have seen in the previous section), its form in the original basis $|\boldsymbol{\xi}^{\mathbf{1R}}\rangle = e^{-\beta E/2}|\boldsymbol{\xi}^{\mathbf{1h}}\rangle$, which encodes the current, is essentially a constant between the two wells.

4.2. States

We have seen in the previous example how in the low temperature limit one can unambiguously define metastable states using the eigenstates of the Fokker-Planck operator. When the energy function is rough, with several non-equivalent minima, or when the origin of metastability is not the low temperature, the construction is less obvious. Suppose the Fokker-Planck spectrum has K eigenstates with low eigenvalues $0, \lambda_1, \ldots, \lambda_{K-1}$, separated by a gap from all the higher ones. One can show[3] that, to the extent that the gap is large ($\lambda_K - \lambda_{K-1} \gg \lambda_{K-1}$), one can construct *exactly* K distributions $P_0(\boldsymbol{x}), \ldots, P_{K-1}(\boldsymbol{x})$ by linear combinations of the right eigenstates of the Fokker-Plank Hamiltonian $\psi^{\alpha R}(\boldsymbol{x})$ with $0 \leqslant \alpha < K$:

$$P_\alpha(\boldsymbol{x}) = \sum_{\gamma=0}^{K-1} T_{\alpha\gamma} \psi^{\gamma R}(\boldsymbol{x}), \tag{38}$$

such that the $P_\alpha(\boldsymbol{x})$ are either positive or negligible, and mutually disjoint (the product of any two is everywhere negligible), these are the *states*. We shall take the $P_\alpha(\boldsymbol{x})$ normalized $\int d^N x\, P_\alpha(\boldsymbol{x}) = 1\ \forall \alpha$. Every combination of the right eigenstates 'below the gap' can be expressed as a linear combination of the states. In particular, the Gibbs measure is:

$$\psi^{0R}(\boldsymbol{x}) = \sum_{\alpha=0}^{K-1} T_{0\alpha}^{-1} P_\alpha(\boldsymbol{x}). \tag{39}$$

A useful formula is obtained integrating (38) with respect to $\boldsymbol{x}$, and noticing that $\langle \boldsymbol{\psi^{0L}} | \boldsymbol{\psi^{\alpha R}} \rangle = 0\ \forall \alpha > 0$:

$$T_{\alpha 0} = 1\ \ \forall \alpha. \tag{40}$$

The left eigenstates 'below the gap' are also interesting. By linear combinations of the left eigenstates $\psi^{\alpha L}(\boldsymbol{x})$ with $0 \leqslant \alpha < K$:

$$A_\alpha(\boldsymbol{x}) = \sum_{\gamma=0}^{K-1} T_{\alpha\gamma} \psi^{\gamma L}(\boldsymbol{x}), \tag{41}$$

one obtains functions $A_\alpha(\boldsymbol{x}), \ldots, A_{K-1}(\boldsymbol{x})$ such that each $A_\alpha(\boldsymbol{x})$ is essentially constant where P_α is non-negligible, and is negligible elsewhere. To summarize, right eigenstates below the gap are locally Gibbsean, while the

corresponding left ones are essentially constant within a 'state'. The case of very low temperatures is the the simplest one to visualize: in this case the P_α are Gaussians sitting each one at the bottom of a local minimum, and the $A_l(\boldsymbol{x})$ are constant within the corresponding (zero temperature) basin of attraction of each minimum, and zero elsewhere.

The low-lying eigenvalues can also be interpreted as exit times. Under the assumption of well separated eigenvalues, their inverses give the exit times corresponding to the metastable states. In fact, the low-lying eigenvalues, together with their corresponding eigenstates will completely define the long-time dynamics of the system. Indeed, one can define, from a probability density $P(\boldsymbol{x})$, the site-populations as

$$c_\gamma = \int d^N x \, A_\gamma(\boldsymbol{x}) P(\boldsymbol{x}), \tag{42}$$

and obtain a master equation for $c_\gamma(t)$ as

$$\frac{dc_\gamma}{dt} = \sum_{\nu=0}^{K-1} w_{\gamma\nu} c_\nu \quad w_{\gamma\nu} = \langle \boldsymbol{A_\gamma} | H_{FP} | \boldsymbol{P_\nu} \rangle. \tag{43}$$

where the metastable distributions are now assumed to be normalized. This master equation is accurate at times for which $\lambda_K e^{-\lambda_K t} \ll \lambda_{K-1} e^{-\lambda_{K-1} t}$.

Let us conclude by mentioning that in cases in which there are more than two separated timescales one can make this construction at more than one level – thus obtaining different sets of states relevant for the different timescales.

4.3. Transition Currents from the 1-Fermion Eigenstates

Let us assume that the Fokker-Planck spectrum has exactly K eigenstates 'below the gap', implying that there are K metastable states. We shall show that, whatever the origin of the gap, exactly as in section 4.1 the $K-1$ one-fermion partners of these eigenstates are the reaction current distributions at long times (for which $\lambda_K e^{-\lambda_K t} \gg \lambda_{K-1} e^{-\lambda_{K-1} t}$). This may seem rather surprising: the construction of states in the previous section is not a priori good in the regions where the probability is negligible. This is not important at the level of the probabilities, as those regions carry vanishingly small weight. However, it seems to pose a problem for the current, which is important on the barrier – in which region the probability corresponding to a state is small – and drops to zero within a state,

precisely where the approximation described in the previous section is reliable. We shall argue now that, in spite of this apparent limitations, as we have already seen in the Section 4.1, the 1-fermion partners give exactly the long-time currents between states.

Let us make the following gedanken-experiment. At time zero we prepare a probability density such that it will fall into one state, say α_o, $0 \leqslant \alpha_o \leqslant K-1$. The initial probability density can then be written as

$$P(\boldsymbol{x}, 0) = \sum_{\alpha=0}^{\infty} c_\alpha \psi^{\alpha R} = c P_{\alpha_o}(\boldsymbol{x}) + \sum_{\alpha \geqslant K} c_\alpha \phi^{\alpha R}. \tag{44}$$

We shall study $P(\boldsymbol{x}, t)$ at a time t in the middle of the gap, that is $\lambda_K t \gg 1 \gg \lambda_{K-1} t$, a time sufficiently large so that all the fast components become very small but not yet large enough as to populate other states. The density is then

$$P(\boldsymbol{x}, t) = c P_{\alpha_o}(\boldsymbol{x}) + O(e^{-\lambda_K t}) + O(1 - e^{-\lambda_{K-1} t}). \tag{45}$$

Let us study now the current

$$J_k = \left(T \frac{\partial}{\partial x_k} + \frac{\partial E}{\partial x_k} \right) P = \sum_{\alpha=1}^{\infty} c_\alpha e^{-\lambda_\alpha t} \left(T \frac{\partial}{\partial x_k} + \frac{\partial E}{\partial x_k} \right) \psi^{\alpha R} = \sum_{\alpha=1}^{\infty} j_k^\alpha, \tag{46}$$

where we have discriminated the contributions to the current of each eigenstate

$$j_k^\alpha \equiv c_\alpha e^{-\lambda_\alpha t} \left(T \frac{\partial}{\partial x_k} + \frac{\partial E}{\partial x_k} \right) \psi^{\alpha R},$$

(using the notations from the previous section and Eq. (45) one can see that $c_\alpha = c T_{\alpha_o \alpha}$). The $\boldsymbol{j}^{\boldsymbol{\alpha}}(\boldsymbol{x})$ are not normalized, so it is difficult to compare them. In order to do so, we compute the divergence of the corresponding terms:

$$\operatorname{div} \boldsymbol{j}^{\boldsymbol{\alpha}}(\boldsymbol{x}) = c_\alpha e^{-\lambda_\alpha t} \lambda_\alpha \psi^{\alpha R}(\boldsymbol{x}). \tag{47}$$

The relative contribution to the current of two terms is of the order:

$$\frac{\int_{\mathcal{V}_\alpha} d^N x \operatorname{div} \boldsymbol{j}^{\boldsymbol{\alpha}}(\boldsymbol{x})}{\int_{\mathcal{V}_\beta} d^N x \operatorname{div} \boldsymbol{j}^{\boldsymbol{\beta}}(\boldsymbol{x})} \propto \frac{c_\alpha \lambda_\alpha}{c_\beta \lambda_\beta} e^{-t(\lambda_\alpha - \lambda_\beta)}, \tag{48}$$

where $\mathcal{V}_\alpha$ and $\mathcal{V}_\alpha$ are the regions in which $\psi^{\alpha R} > 0$, $\psi^{\beta R} > 0$ respectively.[29]

Hence, for large enough times $t(\lambda_\alpha - \lambda_{K-1}) \gg \ln(\frac{c_\alpha \lambda_\alpha}{c_{K-1}\lambda_{K-1}})$, all states α above the gap do not contribute to the current.

In conclusion, we have shown that the escape current of any metastable state is a linear combination of the currents associated to states below the gap. This in turn means that, within this late-time regime, the current is a linear combination of some of the one-fermion eigenstates 'below the gap', those that have zero-fermion partners

$$\int d^N x\, J_k(\boldsymbol{x}) a_k^\dagger |\boldsymbol{x}\rangle \otimes |-\rangle = \mathrm{i} \sum_{\alpha=1}^{K-1} c_\alpha e^{-\lambda_\alpha t} |\boldsymbol{\xi}^{\boldsymbol{\alpha R}}\rangle = \mathrm{i} \sum_{\alpha=1}^{K-1} c_\alpha e^{-\lambda_\alpha t} \bar{Q} |\boldsymbol{\psi}^{\boldsymbol{\alpha R}}\rangle. \quad (49)$$

In the next section we interpret those having a two-fermion partner.

4.3.1. Transition Times

Suppose one has the current $\boldsymbol{J}$ escaping a metastable state $P(\boldsymbol{x})$:

$$J_i(\boldsymbol{x}) \propto \left(T \frac{\partial}{\partial x_i} + E_{,i} \right) P(\boldsymbol{x}) \;\; ; \;\; P(\boldsymbol{x}) = \sum_{\alpha=1}^{K-1} c_\alpha \psi^{\alpha R}(\boldsymbol{x}). \quad (50)$$

We wish to give an expression for the transition time in terms of the unnormalized current $\boldsymbol{J}$. For this, we first compute:

$$\begin{aligned} \int d^N x\, e^{\beta E}\, \boldsymbol{J}^2 &= \int d^N x \left\{ \left(T \frac{\partial}{\partial x_i} + E_{,i} \right) P \right\} e^{\beta E} \left\{ \left(T \frac{\partial}{\partial x_i} + E_{,i} \right) P \right\} \\ &= \int d^N x \left\{ \left(T \frac{\partial}{\partial x_i} + E_{,i} \right) P \right\} \frac{\partial}{\partial x_i} \left(e^{\beta E} P \right) \\ &= \int d^N x\, P\, e^{\beta E} H_{FP} P = \sum_{\alpha=1}^{K-1} \lambda_\alpha c_\alpha^2, \end{aligned} \quad (51)$$

and similarly:

$$\int d^N x\, e^{\beta E} (\mathrm{div}\, \boldsymbol{J})^2 = \int d^N x\, (H_{FP} P)\, e^{\beta E}\, (H_{FP} P) = \sum_{\alpha=1}^{K-1} \lambda_\alpha^2 c_\alpha^2, \quad (52)$$

because the sums are dominated by the largest eigenvalues λ_{max} within the sum (52) that contribute to the state $P(\boldsymbol{x})$, we have that the smallest escape time is:

$$t_{activ} = \lambda_{max}^{-1} = \frac{\int d^N x\, e^{\beta E}\, \boldsymbol{J}^2}{\int d^N x\, e^{\beta E}\, (\mathrm{div}\, \boldsymbol{J})^2}. \tag{53}$$

Note that the normalization of the current is irrelevant. *This formula is valid on the assumption of separation of timescales, irrespective of its cause.* The Kramers expression for the low-temperature case can be easily read of this formula, since the numerator is dominated by the exponential of the barrier height and the denominator by the exponential of the energy of the starting well. If the current is divergence-less (a loop, as we shall encounter later), the timescale is infinite.

An immediate conclusion one draws from Eq. (53) is that if one knows the current with an error $\delta \boldsymbol{J}(\boldsymbol{x})$, it is in the regions with large energy (the saddles) and with large divergence (the starting region) where this error translates into a larger error in the timescale.

4.4. Loops: Blind Saddles and Subdominant Paths

The one-fermion sector contains in general two kinds of eigenstates states 'below the gap'. These are those given by $\bar{Q}$ acting on a zero-fermion state, and those given by Q acting on a two-fermion state. The former give us the dominant reaction currents, as we have seen already. We now show that the latter give us current loops, and in particular the the alternative (subdominant) routes between states.

The states we are now considering are constructed as follows: given a two-fermion eigenstate $|\boldsymbol{\rho}^{\boldsymbol{R}}\rangle = \sum_{ij=1}^{N} a_i^\dagger a_j^\dagger |\rho_{ij}^R\rangle$, we obtain a one-fermion eigenstate as:

$$Q|\boldsymbol{\rho}^{\boldsymbol{R}}\rangle \equiv |\boldsymbol{\chi}^{\boldsymbol{R}}\rangle = \sum_{i=1}^{N} a_i^\dagger |\chi_i^R\rangle \otimes |-\rangle; \quad \chi_i^R(\boldsymbol{x}) = -\mathrm{i}T \sum_{j=1}^{N} \left(\frac{\partial \rho_{ij}^R}{\partial x_j} - \frac{\partial \rho_{ji}^R}{\partial x_j} \right), \tag{54}$$

unless $|\chi_i^R\rangle = 0$. From $Q|\boldsymbol{\chi}^{\boldsymbol{R}}\rangle = 0$ we immediately conclude that field of the right eigenstate is divergenceless:

$$\sum_{i=1}^{N} \frac{\partial \chi_i^R(\boldsymbol{x})}{\partial x_i} = 0. \tag{55}$$

so that if $|\boldsymbol{\chi}^{\boldsymbol{R}}\rangle$ encodes a single current line, it must be a closed loop.

4.4.1. Simple Examples

A low temperature example will make things clearer. Consider the tilted Mexican hat in two dimensions (Fig. 4): it has a minimum, a maximum, and a 'blind' saddle, one that does not lead anywhere. The two-fermion lowest eigenstate is of the form

$$|\boldsymbol{\rho}^{\boldsymbol{R}}\rangle = a_x^\dagger a_y^\dagger |\rho^R\rangle \otimes |-\rangle, \tag{56}$$

where $\rho^R(x, y)$ satisfies:

$$-\left(T\frac{\partial}{\partial x}+\frac{\partial E}{\partial x}\right)\frac{\partial}{\partial x}\rho^R(x, y)-\left(T\frac{\partial}{\partial y}+\frac{\partial E}{\partial y}\right)\frac{\partial}{\partial y}\rho^R(x, y)=\lambda\rho^R(x, y), \tag{57}$$

which is easily obtained permuting (fermion) particles and holes in the Hamiltonian (13). The lowest-lying one-fermion eigenstate is obtained by noticing that the eigenvalue equation (57) corresponds to the equation satisfied by the *left* eigenstate of a Fokker-Planck equation in a the reversed potential $-E(x, y)$ (cfr. Eq. (20)). From the discussion in Section4, we conclude that ρ^R (the only $A(x, y)$ for the reversed problem) is essentially constant within the region spanned by all gradient lines descending from the local maximum (the unstable manifold of the maximum, or the stable manifold of the minimum of $-E$) – and drops sharply to zero at the border of this region. Acting with Q on ρ^R, we obtain the current:

$$\left(\chi_x^R(x, y), \chi_y^R(x, y)\right) \sim \left(\frac{\partial \rho^R}{\partial y}, -\frac{\partial \rho^R}{\partial x}\right), \tag{58}$$

which is then non-negligible on the gradient paths joining the minimum with the saddle, because this is where ρ^R has a non-negligible gradient. The direction is turnaround, and clearly the flow so obtained is divergence-free.

Let us now see the general relation between passages and loops with another slightly more complicated low temperature example. Consider a situation as in Fig. 5. There are four minima, multiply connected by seven paths going through as many saddles. At low temperature, only three of them (shown in thicker lines) have a much shorter passage time, and hence dominate the reactions. The other four can be obtained from combination of these and the four independent loops — for example one can take each loop going around each of the four maxima. The eigenstate struc-

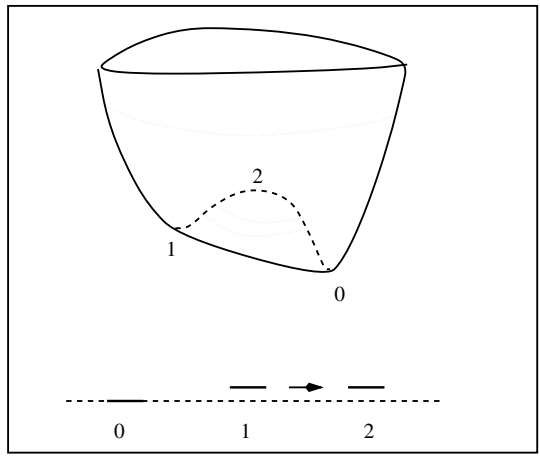

Fig. 4. A landscape with a minimum, a maximum and a blind saddle. Below: the low eigenvalue spectrum for zero, one and two fermions. The dotted line is the zero level, other eigenvalues are exponentially small in $1/T$. Next higher eigenvalues start at $O(1)$ (not shown).

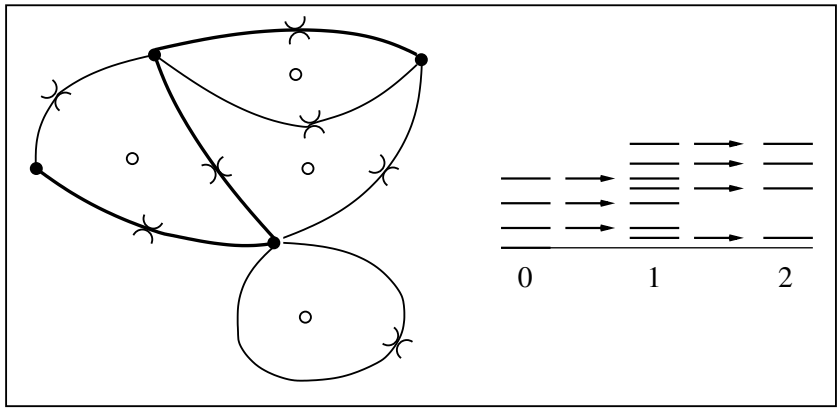

Fig. 5. A sketch of an energy surface with four minima (full circles), four maxima (open circles) and seven pathways passing through one saddles. The thick paths have a low activation times. On the right the corresponding spectrum of the Hamiltonian (13).

ture 'below the gap' reflects this: there are four zero-fermion (right) eigenstates corresponding to four minima. One of them is the Gibbs measure, the other three have one-fermion partners yielding the three dominant passages. The remaining four one-fermion (right) eigenstates correspond to the loops, and they have two-fermion partners corresponding to the regions they encircle, including each a maximum.

The simple tilted Mexican hat problem, and in general any two-dimensional situation, allows us also to understand the different roles played by partner eigenstates below the gap in the one and two fermion subspaces. As we have mentioned above, all the right two-fermion eigenstates which are partners to the loops can be obtained (always in two dimensions) from the zero-fermion left eigenstate of the inverted potential. This means that each corresponds to a constant in the region spanned by all trajectories descending from a saddle of index two (its unstable manifold), and this will be also true in more dimensions.

4.4.2. Loops: Physical Meaning and Derivations

The loops have also a physical meaning which may be extended to apply to the nonzero temperature situation. Consider a system in equilibrium to which we add a force field $h\boldsymbol{f}(\boldsymbol{x})$, h small, that has only rotational in a restricted region $\mathcal{D}_\Gamma$ of phase space:

$$\frac{\partial f_j}{\partial x_k} - \frac{\partial f_k}{\partial x_j} = 0 \ \forall j,k \text{ if } \boldsymbol{x} \notin \mathcal{D}_\Gamma. \tag{59}$$

The effect of such a field will be to create currents which will persist even in the stationary state. In a system with metastability, these currents can be of two types: those generated essentially within a state, and those due to forced passages through barriers; the latter are the loops. We shall see that the currents within a state are given by eigenstates above, and the loops by eigenstates below the gap of the one-fermion spectrum.

To make this clear let us go back to the tilted Mexican hat (Fig. 6). Let us consider a force whose rotational is concentrated in a restricted 'vorticity' region $\mathcal{D}_\Gamma$ (the dark region in the figure). If the vorticity is concentrated close to the minimum (6a) the currents generated will be due to particles which in a rare excursion happen to fall upon $\mathcal{D}_\Gamma$, and then typically fall right back to the state. If we shift the $\mathcal{D}_\Gamma$ further away from the state, we get a behavior of the same kind until we reach a point in which the vorticity is located higher than the saddle point, and it becomes more probable for the current to go round the saddle (6b) through gradient lines: this is the loop distribution and is essentially independent of the exact position of $\mathcal{D}_\Gamma$. It is given by the (only) one-fermion eigenstate below the gap. As we shall see below, the condition that the vorticity generates a loop around a saddle is that it pierces the surface on which the two-fermion eigenstate 'below the gap' is non-zero: this is a general fact.

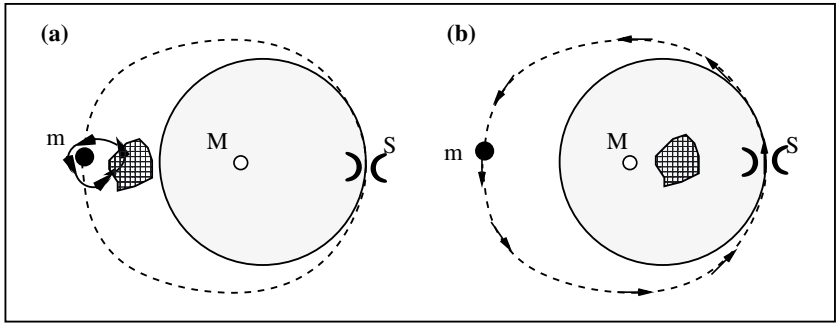

Fig. 6. The tilted Mexican hat seen from above. The full lines are the level lines at the energy of the saddle (S): the light gray region is above the saddle level. The broken line corresponds to the gradient line going from the minimum (m), through the saddle, and back to the minimum encircling the maximum (M). The dark gray region corresponds to the domain $\mathcal{D}_\Gamma$ where the drift has a non-zero vorticity. Left: $\mathcal{D}_\Gamma$ below the saddle level - currents above the gap; Right: $\mathcal{D}_\Gamma$ above the saddle level - currents below the gap. See text.

In order to see this quantitatively, let us study the perturbed Fokker-Planck equation:

$$H_{FP}^{f} = -\sum_{i=1}^{N} \frac{\partial}{\partial x_i}\left(T\frac{\partial}{\partial x_i} + E_{,i} + hf_i\right), \tag{60}$$

with h a small parameter and f_i as above. Proposing a stationary distribution of the form:

$$H_{FP}^{f} P_{st} = 0 \;;\; P_{st} = c_o e^{-\beta E} + hP^1, \tag{61}$$

(c_o the normalization of the Gibbs measure) the current in the stationary state is obtained as:

$$\begin{aligned} J_i^{st} &= \left(T\frac{\partial}{\partial x_i} + E_{,i} + hf_i\right) P_{st} = h\left[c_o f_i e^{-\beta E} + \left(T\frac{\partial}{\partial x_i} + E_{,i}\right) P^1\right] \\ &= he^{-\beta E}\left[c_o f_i + T\frac{\partial}{\partial x_i}\left(e^{\beta E} P^1\right)\right], \end{aligned} \tag{62}$$

and is zero only if the square bracket vanishes, i.e. if $\boldsymbol{f}$ derives from a potential. The current is obviously divergence-free, and it is easy to see

that the corresponding one-fermion state $|\boldsymbol{\xi}^{\boldsymbol{R}}\rangle = \int d^N x \sum_{i=1}^N J_i^{st}(\boldsymbol{x}) a_i^\dagger |\boldsymbol{x}\rangle \otimes |-\rangle$ satisfies:

$$Q|\boldsymbol{\xi}^{\boldsymbol{R}}\rangle = 0, \tag{63}$$

$$\bar{Q}|\boldsymbol{\xi}^{\boldsymbol{R}}\rangle = c_o h T e^{-\beta E}|\boldsymbol{\Gamma}\rangle, \tag{64}$$

where

$$|\boldsymbol{\Gamma}\rangle = -\mathrm{i}\left(\frac{\partial f_j}{\partial x_k} - \frac{\partial f_k}{\partial x_j}\right) a_j^\dagger a_k^\dagger |-\rangle. \tag{65}$$

Equation (63) implies that $|\boldsymbol{\xi}^{\boldsymbol{R}}\rangle$ can be developed in terms of one-fermion eigenstates with two-fermion partners. Multiplying the Eq. (64) by Q, we obtain:

$$|\boldsymbol{\xi}^{\boldsymbol{R}}\rangle = c_o h H^{'-1} Q e^{-\beta E}|\boldsymbol{\Gamma}\rangle = c_o h\, H^{'-1} e^{-\beta E}\bar{Q}^\dagger|\boldsymbol{\Gamma}\rangle, \tag{66}$$

where H' is H restricted to the one-fermion subspace. Developing (66) in a basis, we find:

$$|\boldsymbol{\xi}^{\boldsymbol{R}}\rangle = c_o h \sum_\alpha \frac{1}{\lambda_\alpha}|\boldsymbol{\xi}^{\boldsymbol{\alpha R}}\rangle\langle\Gamma|\bar{Q}|\boldsymbol{\xi}^{\boldsymbol{\alpha R}}\rangle. \tag{67}$$

Defining as H_+ and H_- the projections of H' above and below the gap, respectively, we introduce the components of the current distribution:

$$\begin{aligned} |\boldsymbol{\xi}^{\boldsymbol{R}}_{\boldsymbol{state}}\rangle &= c_o h H_+^{-1} e^{-\beta E}\bar{Q}^\dagger|\boldsymbol{\Gamma}\rangle, \\ |\boldsymbol{\xi}^{\boldsymbol{R}}_{\boldsymbol{tour}}\rangle &= c_o h H_-^{-1} e^{-\beta E}\bar{Q}^\dagger|\boldsymbol{\Gamma}\rangle. \end{aligned} \tag{68}$$

We can bound:

$$\begin{aligned} \| |\boldsymbol{\xi}^{\boldsymbol{R}}_{\boldsymbol{state}}\rangle \|^2 &= (c_o h)^2 \langle\boldsymbol{\Gamma}|\bar{Q}e^{-\beta E} H_+^{-1\dagger} H_+^{-1} e^{-\beta E}\bar{Q}^\dagger|\boldsymbol{\Gamma}\rangle \\ &\leqslant \lambda_{+min}^{-2}\,(c_o h)^2\,\langle\boldsymbol{\Gamma}|\bar{Q}e^{-2\beta E}\bar{Q}^\dagger|\boldsymbol{\Gamma}\rangle, \end{aligned} \tag{69}$$

where λ_{+min} is the smallest eigenvalue of H in the one-fermion subspace above the gap and we have used $\langle\psi|AA^\dagger|\psi\rangle \leqslant |\alpha_{max}|^2\langle\psi|\psi\rangle$, with $|\alpha_{max}|$ the maximal eigenvalue of A. As $\langle\boldsymbol{x}|\bar{Q}^\dagger|\boldsymbol{\Gamma}\rangle$ is nonzero only in the rotational region $\mathcal{D}_\Gamma$ where it can be taken of order one, in the low temperature limit $\langle\boldsymbol{\Gamma}|\bar{Q}e^{-2\beta E}\bar{Q}^\dagger|\boldsymbol{\Gamma}\rangle^{1/2} \sim e^{-\beta E_\Gamma}$ where $E_\Gamma = min\{E(\boldsymbol{x})|\boldsymbol{x} \in \mathcal{D}_\Gamma\}$. Given that λ_{+min}^{-2} is of order one and c_o is the normalization of

the Gibbs distribution, the contribution above the gap will bounded as $\|\xi^{\mathbf{R}}_{\mathbf{state}}\rangle\| \leqslant c_o e^{-\beta E_\Gamma} \sim e^{-\beta(E_\Gamma - E_{min})}$, exactly what we expect of a process that starts in a minimum and climbs up to the region $\mathcal{D}_\Gamma$ of energy E_Γ where the vorticity is important, and falls back again.

The contribution of eigenstates below the gap is instead given by the loops, a fact we shall show in general in the low temperature limit. The physical meaning of the two-fermion wave functions below the gap $|\chi^{\alpha}\rangle \equiv \bar{Q}|\xi^{\alpha R}\rangle$, is now clear from Eq. (67): the factor $\langle \Gamma|\bar{Q}|\xi^{\alpha R}\rangle$ will be important only if the 'vorticity' Γ intersects the region where the two-fermion eigenstate $|\chi^{\alpha}\rangle \equiv \bar{Q}|\xi^{\alpha R}\rangle$ is non-negligible. Hence, each two-fermion partner of a one-fermion eigenstate below the gap defines the region where a vorticity has to be applied in order to excite a current through the corresponding loop. In the low temperature case, one expects the current through the saddle to be of order $e^{\beta(E_{saddle}-E_{min})}$. If $E_\Gamma > E_{saddle}$ the contribution of the loops dominate, and the bound above means that it can only be given by the eigenstates below the gap. Since in simple systems there are only a few of those, the distribution will not change dramatically with small changes of the vorticity location.

In the general case of systems with a gap in timescale, but with non-zero temperature, one can still consider forces whose vorticity is 'near' or 'far' from a state, and computing the currents induced one can take the construction as a basis for a definition of 'loop'. An interesting question is to analyze the effect these loops have in the series development of the free energy, an analysis à la Langer[2] would clarify the issue.

4.5. Induced Currents and Holes

One of the cases in which it is interesting to calculate currents is when we apply a constant electric field and join the ends of the sample. We create thus a manifold with a hole inside. Up to now we have excluded such situations, and indeed some modifications to the arguments have to be taken into account. Consider the simple example of a particle in a one-dimensional ring with coordinate x, with $0 \leqslant x \leqslant 2\pi$, and no potential. Both the Fokker-Planck and supersymmetric operators read:

$$H = \frac{1}{T}(Q + \bar{Q})^2 = -T\frac{\partial^2}{\partial x^2} = H_{FP}, \tag{70}$$

with

$$Q = -\mathrm{i}T\frac{\partial}{\partial x}a \;\; ; \;\; \bar{Q} = -\mathrm{i}T\frac{\partial}{\partial x}a^{\dagger}. \tag{71}$$

The zero fermion states are $\propto e^{ikx}$, with k any integer. In particular, the zero-fermion ground state is a constant, $\psi^{0R}(x) = \frac{1}{2\pi}$ as expected. On the other hand, one-fermion states are also of the form $\propto e^{ikx} a^\dagger|-\rangle$: we find that we have a one-fermion eigenstate with zero eigenvalue $|\boldsymbol{\xi}^{\boldsymbol{0R}}\rangle = \frac{1}{2\pi} a^\dagger|-\rangle$, a possibility that we had excluded for spaces without holes (see Appendix A). Furthermore, the one-fermion ground state has no partner: $|\boldsymbol{\xi}^{\boldsymbol{0R}}\rangle \neq \bar{Q}|\boldsymbol{\psi}^{\boldsymbol{R}}\rangle$. The situation changes when we add a constant field $\mathcal{E}$, so that now:

$$H = \frac{1}{T}(Q + \bar{Q}_{\mathcal{E}})^2 = -\frac{\partial}{\partial x}(T\frac{\partial}{\partial x} + \mathcal{E}) = H_{FP}, \tag{72}$$

with

$$Q = -\mathrm{i}T\frac{\partial}{\partial x}a;\ \bar{Q}_{\mathcal{E}} = -\mathrm{i}(T\frac{\partial}{\partial x} + \mathcal{E})a^\dagger. \tag{73}$$

The eigenstates do not change, and we still have the same one and zero-fermion ground states, but now, remarkably:

$$-\mathrm{i}\mathcal{E}|\boldsymbol{\xi}^{\boldsymbol{0R}}\rangle = \bar{Q}_{\mathcal{E}}|\boldsymbol{\psi}^{\boldsymbol{0R}}\rangle \neq 0, \tag{74}$$

so that one and zero fermion ground states have become partners. We also conclude that the meaning of the one-fermion ground state is to give the stationary current distribution around the ring. A last point to see in this simple example is that when the field is on, the force does not derive globally from a potential ($E = \mathcal{E}x$ would be multiply valued), and we cannot change globally to the Hermitian basis!

Consider in general diffusion in a space with a hole, so that we can have a force field $\boldsymbol{f}$ with everywhere $\frac{\partial f_j}{\partial x_i} = \frac{\partial f_i}{\partial x_j}$ but *not* deriving from a global potential. We consider a small perturbation

$$H^f_{FP} = -\sum_{i=1}^{N} \frac{\partial}{\partial x_i}\left(T\frac{\partial}{\partial x_i} + E_{,i} + hf_i\right), \tag{75}$$

with h a small parameter. Proposing as before a stationary distribution of the form: $P_{st} = c_o e^{-\beta E} + hP^1$ the current in the stationary state is again given by (62). It is easy to see that the corresponding one-fermion state $|\boldsymbol{\xi}^{\boldsymbol{R}}\rangle = -\mathrm{i}\int d^N x \sum_{i=1}^{N} J_i^{st}(\boldsymbol{x}) a_i^\dagger|\boldsymbol{x}\rangle \otimes |-\rangle$ now satisfies:

$$Q|\boldsymbol{\xi}^{\boldsymbol{R}}\rangle = 0, \quad \bar{Q}|\boldsymbol{\xi}^{\boldsymbol{R}}\rangle = 0. \tag{76}$$

Also:

$$|\boldsymbol{\xi}^{\boldsymbol{R}}\rangle = \bar{Q}_f|\boldsymbol{P_{st}}\rangle = -\mathrm{i}\left[T\frac{\partial}{\partial x_i} + E_i + hf_i\right]|\boldsymbol{P_{st}}\rangle$$
$$= -\mathrm{i}he^{-\beta E}\sum_{i=1}^{N} a_i^{\dagger}\left[c_o f_i + T\frac{\partial\left(e^{\beta E}P_1\right)}{\partial x_i}\right]|-\rangle. \tag{77}$$

Just as in the previous example, we have shown that it is the nonconservative field that makes $|P_{st}\rangle$ and $|\boldsymbol{\xi}^{\boldsymbol{R}}\rangle$ become partners (otherwise the last of (77) is empty), and the physical interpretation is that each zero eigenvalue one-fermion eigenstate corresponds to a current induced around a hole by small fields. Again, for the perturbed Hamiltonian H_{FP}^{f} one cannot construct a global Hermitian basis as for H_{FP}.

Let us conclude this section with an alternative variational interpretation for the loops. Suppose we ask which is the field $\boldsymbol{f}$ such that it maximizes the power $W = \int d^N x \sum_{i=1}^{N} f_i J_i^{st}$ done on the system, while having the minimal Gibbs expectation V for its violation of detailed balance (the 'vorticity'):

$$V \equiv \frac{\int d^N x\, e^{-\beta E}\sum_{jk=1}^{N}\left(\frac{\partial f_j}{\partial x_k} - \frac{\partial f_k}{\partial x_j}\right)^2}{\int d^N x\, e^{-\beta E}}. \tag{78}$$

A simple calculation using (64) yields:

$$\mathcal{F} = \frac{V}{W} \propto \frac{\sum_{\alpha \geqslant 1} c_\alpha^2 \lambda_\alpha}{\sum_{\alpha \geqslant 1} c_\alpha^2}, \tag{79}$$

where $c_\alpha = \int d^N x \sum_{k=1}^{N} f_k \xi_k^{\alpha R}$ and $|\boldsymbol{\xi}^{\boldsymbol{\alpha R}}\rangle$ are 1-fermion eigenstates annihilated by Q (the 'loops'). In conclusion $\mathcal{F}$ is minimized if $\mathbf{f}$ is a left, 1-fermion eigenstate 'below the gap'. Clearly, the definition is valid at arbitrary temperatures.

5. THE BIG PICTURE

5.1. Low Temperature Structures

At low temperatures eigenstates peak on structures with dimensions smaller than N, and fall of exponentially away from them, in a width that vanishes with T. Right eigenstates 'below the gap' are made of linear combinations of functions peaked on the following structures:

- *Zero fermions*: points, the local minima.
- *One fermion*: gradient lines joining minima through saddle points. The eigenstates with a zero-fermion partner are the true, open paths, and those with two-fermion partners are closed loops.
- *Two fermions*: Two-dimensional surfaces containing a saddle with two unstable directions, spanned by all the descending gradient lines emanating from it. The eigenstates with a one-fermion partner are peaked on open surfaces (surfaces with borders), and those with three-fermion partners are peaked on closed surfaces (borderless surfaces).

The physical property of the open surfaces is that a weak nonconservative field $\boldsymbol{f}$ will generate a current turning around their border, and this only if the 'vorticity' region in which $\left(\frac{\partial f_j}{\partial x_i} - \frac{\partial f_i}{\partial x_j}\right) \neq 0$ intersects them.

- *k fermions*: k-dimensional surfaces containing a saddle of index k, spanned by all gradient lines descending from it (the unstable manifold of the saddle).

Again, the eigenstates with $k-1$ fermion partners are peaked on open, and those with $k+1$-fermion partners on closed surfaces. The border of the surface associated with the former is the region where the $k-1$ fermion partners are peaked.

Left eigenstates 'below the gap' can be obtained using the fact that a left eigenstate with k fermions is a *right* $N-k$ fermion eigenstate of the problem with the inverted potential $-E$ (cfr. Eq. (20)).

One thus concludes that k fermion left eigenstates are made of linear combinations of functions peaked on the following structures:

- *Zero fermions*: constant within a basin of attraction of each minimum (a well known fact).
- *One fermion*: $N-1$ dimensional basin of attractions of saddles (themselves subsets of the borders between basins).
- *Two fermions*: $N-2$ dimensional basins of attraction of saddles with two unstable directions.
- *k fermions*: $N-k$-dimensional surfaces spanned by the set of descending paths terminating in each saddle of index k (i.e., the basins of attractions of these saddles).

This is the structure of basins within basins that was argued is relevant in systems with slow dynamics.[30] One can again distinguish open and closed surfaces, and this is related to whether the wave function of k fermions has a partner with $k-1$ or $k+1$ fermions.

Each of the right eigenstates below the gap are peaked on unstable manifolds of the corresponding critical point, while the left eigenstates are peaked on the stable manifolds. In this frame, the $\bar{Q}$ and Q operators act

as 'boundary operators' generating what is called in the mathematical literature the Morse (co)homology. We shall derive these results constructively in the next section.

A simple, three-dimensional example will illustrate this. Consider the energy $E(x, y, z) = e(x) + e(y) + e(z)$, where $e(x_i)$ is the symmetric double-well potential of Fig. 3. The landscape is defined by a cube with minima in its 8 vertexes, 12 saddles of index 1 midway along its sides, 6 saddles of index 2 at the face centers and one saddle of index 3 at the cube's center. The right eigenstates below the gap are as follows *i*) 8 with zero fermions located at the vertices's, *ii*) 12 with one fermion located on the sides, of which seven are passages and five are loops along the perimeter of the faces, *iii*) 6 with two fermions peaked on the faces, of which five are independent open faces and one is the total (closed) surface of the cube, and *iv*) one with three fermions constant inside all the interior of the cube.

5.2. Defining 'Free energy' Structures

The zero-temperature limit allows us to see very clearly the different structures that emerge. However, the main point of this paper is that these can be transferred to a more general situation, provided that there is timescale separation – whatever its origin. As we have seen already, the role of local minima in the low-temperature situation is taken by metastable states, and the role of gradient lines by reaction current distributions. In the previous section we also attempted a general definition of 'reaction loop', on the basis of the currents that can be induced by a non-conservative weak force. One has the possibility of also defining higher structures associated with fermion subspaces of higher fermion numbers, (like borders, basins etc.) in general. In problems in which one can define a free-energy landscape in a precise way (typically mean-fieldish situations), the structures we have defined should recover their geometric appearance: states becoming points, reaction distributions becoming lines, etc, but now in the free-energy landscape, in which each point stands for many configurations. The importance of the construction we have been describing is that it does not rely on such a landscape: the only assumption is timescale separation. Once this is given, the Morse-theory constraints on the objects follow automatically, thus showing that the construction makes geometric sense. We shall also see in what follows how these structures are be approached by higher forms of stochastic equations.

6. DIFFUSION DYNAMICS

6.1. Dynamics

In order to obtain the currents we must find eigenstates of the supersymmetric Hamiltonian (13) 'below the gap' in the 1-fermion sector. This may be achieved by solving Eq. (6) at times larger than the microscopic times starting from several initial configurations. In the zero-fermion case, one in fact simulates the Langevin dynamics (1) rather than solving the Fokker-Plank equation, in order to obtain metastable states. The question naturally arises as to which is the diffusion equation that reproduces Eq. (6) in the one fermion subspace, and more generally in any K-fermion subspace.[31]

Let us do this for one-fermion wave functions first.

Consider first one particle carrying an N-component vector degree of freedom $\boldsymbol{u}$. Let the position of the particle evolve as a Langevin process (1), and the vector $\boldsymbol{u}$ as:

$$\dot{u}_i = -\sum_{j=1}^{N} E_{ij}(\boldsymbol{x}) u_j. \tag{80}$$

From Eqs. (1) and (80), we have that the joint distribution function $\tilde{F}(\boldsymbol{x}, \boldsymbol{u}, t)$ evolves then as:

$$\frac{\partial \tilde{F}(\boldsymbol{x}, \boldsymbol{u}, t)}{\partial t} = \left[-H_{FP} + \sum_{ij=1}^{N} \frac{\partial}{\partial u_i} E_{,ij} u_j \right] \tilde{F}(\boldsymbol{x}, \boldsymbol{u}, t). \tag{81}$$

Consider now the evolution of the partial averages:

$$R_a(\boldsymbol{x}, t) = \int d^N u \, u_a \, F(\boldsymbol{x}, \boldsymbol{u}, t), \tag{82}$$

$$\begin{aligned} \frac{\partial R_a(\boldsymbol{x}, t)}{\partial t} &= \int d^N u \, u_a \frac{\partial \tilde{F}(\boldsymbol{x}, \boldsymbol{u}, t)}{\partial t} \\ &= \int d^N u \, u_a \left[-H_{FP} + \sum_{ij=1}^{N} \frac{\partial}{\partial u_i} E_{,ij} u_j \right] \tilde{F}(\boldsymbol{x}, \boldsymbol{u}, t) \\ &= -H_{FP} R_a(\boldsymbol{x}, t) - \sum_{j=1}^{N} E_{aj} R_j(\boldsymbol{x}, t), \end{aligned} \tag{83}$$

where we have integrated by parts on u_a. This is Eq. (7), as announced.

The evolution as in Eqs. (80) and (81) has the problem that the particle may very rarely visit a given region of space, but once it does so have large components for $\boldsymbol{u}$. A practical modification is to preserve the norm of the vector attached to the particle. Putting $\boldsymbol{v} \equiv \boldsymbol{u}/|\boldsymbol{u}|$ we obtain the following equation for a function $F(\boldsymbol{x}, \boldsymbol{v}, t)$:

$$\frac{\partial F(\boldsymbol{x}, \boldsymbol{v}, t)}{\partial t} = \left[-H_{FP} + \sum_{ij=1}^{N} \frac{\partial}{\partial v_i} \left\{ E_{,ij} v_j - v_i \sum_{kl=1}^{N} v_k v_l E_{kl} \right\} - \sum_{kl=1}^{N} v_k v_l E_{kl} \right] F(\boldsymbol{x}, \boldsymbol{v}, t). \tag{84}$$

Computing the evolution of the partial averages

$$R_a(\boldsymbol{x}, t) = \int_{|\boldsymbol{v}|^2=1} d\boldsymbol{v}\, v_a\, F(\boldsymbol{x}, \boldsymbol{v}, t), \tag{85}$$

the result is again Eq. (7). The diffusional process involved is however quite different. The first term in the square bracket in Eq. (84) tells us that the dynamics of the particle is still of the Langevin form. The second term now gives for the evolution of $\boldsymbol{v}$:

$$\dot{v}_i = -\sum_{j=1}^{N} E_{ij}(\boldsymbol{x}) v_j + v_i \sum_{kl=1}^{N} v_k v_l E_{kl}, \tag{86}$$

which preserves the condition $\| \boldsymbol{v} \| = 1$. The third in (84) is a 'cloning' term, creating and destroying particles at a rate $\sum_{kl=1}^{N} v_k v_l E_{kl}$.[33] In Fig. 7 we show the numerical solution of the diffusion equation for vector walkers in a potential.

6.2. Low Temperature Structures

Let us now use the equations for $\boldsymbol{v}$ to show that at low temperatures the eigenstates with eigenvalues close to zero correspond to lines joining minima through the saddles. At low temperatures, particles fall along gradient lines:

$$\dot{x}_i = -E_{,i}(x). \tag{87}$$

Assume that the distribution consists of particles sitting along an isolated gradient line, and having $v_i = E_i/|\nabla E|$. Putting this into (86), we find that

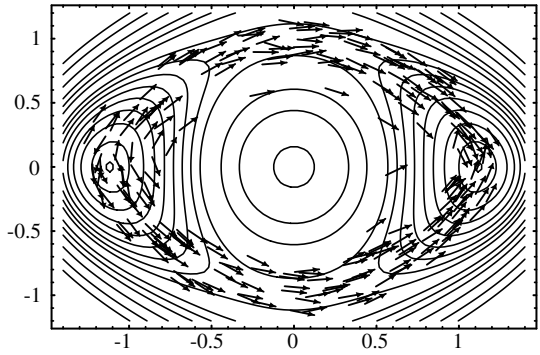

Fig. 7. Snapshot of a population of walkers in the stationary state. The potential is taken from.[37] It has two minima (right and left), two saddles (top and bottom) and a maximum in the center.

the condition $v_i = E_i/|\nabla E|$ is preserved as particles fall along the gradient line. On the other hand, the depletion of particles along the trajectory consists of a term due to migration $-\frac{d\dot{x}_\ell}{d\ell} = \frac{d\nabla \boldsymbol{E}\cdot\boldsymbol{v}}{d\ell}$ ($d\ell$ the element length along the line), and of cloning $\sum_{kl=1}^{N} v_k v_l E_{kl}$: both terms cancel since $d\ell$ is parallel to $\boldsymbol{v}$. Hence, a uniform distribution of particles along a gradient line with $v_i = E_i/|\nabla E|$ is stable, provided nothing happens at the ends. Now, the only possibility for the ends not to destroy stability is that they are stationary points, so that there is no particle exchange there. Furthermore, the distribution has to be in particular peaked along a path joining two minima through a saddle of order one. The reason is as follows: particles are constantly falling, the measure is preserved because there is a high birth rate near the saddle. Now, if the saddle in question is of index higher than one, the slightest noise will make particles that are born near it emigrate in other directions, as there is more than a single descent path in that case, rendering the solution along a single gradient line unstable. Also, if $d\ell$ and $\boldsymbol{v}$ are not initially parallel, they will become so only on the saddle of index one. A stable one-fermion solution on a higher dimensional surface is on the other hand impossible because the surface expansion rate is no longer compensated by the cloning.

In Appendix C we give the generalization of the evolution equations for higher fermion numbers, and we use them to generalize this argument to show the result announced in the previous section that low-temperature k-fermion eigenvalues below the gap are linear combinations of constant densities filling the surfaces spanned by all the descending paths emanating from saddles of order k. The argument is entirely similar to the one for the one-fermion sector: each particle has a k-form

attached to it, whose distribution is preserved as it falls down. The cloning term precisely compensates the effect of the redistribution of particles, and the solution for k forms is unstable unless particles are born near a saddle of index k.

6.3. Long-Time Evolution of v

At times longer than the inverse of the lowest one-fermion eigenvalue, one can expect that $F(\boldsymbol{x}, \boldsymbol{v}, t)$ will converge to a stationary distribution symmetric in $\boldsymbol{v}$:

$$\lim_{t\to\infty} F(\boldsymbol{x}, \boldsymbol{v}, t) = F^{eq}(\boldsymbol{x}, \boldsymbol{v}), \qquad F^{eq}(\boldsymbol{x}, \boldsymbol{v}) = F^{eq}(\boldsymbol{x}, -\boldsymbol{v}) \quad \forall \boldsymbol{v}, \tag{88}$$

and the averages (85) vanish

$$R_a^{eq}(\boldsymbol{x}, t) = \int_{|\boldsymbol{v}|^2=1} d^N v \; v_a \, F^{eq}(\boldsymbol{x}, \boldsymbol{v}, t) = 0. \tag{89}$$

To compensate the mean death rate, the usual practice in Diffusion Monte Carlo schemes is to add an overall cloning probability (see ref. 33). In any case, one can show that $F^{eq}(\boldsymbol{x}, \boldsymbol{v})$ itself will be peaked on paths at low temperatures. To do this, it suffices remake the argument of Section 5.1.

7. PATH SAMPLING: LYAPUNOV WEIGHTS

The same ideas can be written in the path-integral formalism. Let us start by computing

$$\begin{aligned} I(\boldsymbol{x_0}, \boldsymbol{x_1}) &= \sum_{i=1}^{N} \langle - | \otimes \langle \boldsymbol{x_0} | a_i \, e^{-Ht} \, a_i^\dagger | \boldsymbol{x_1} \rangle \otimes | - \rangle \\ &= \sum_{\alpha \geqslant 1} \sum_{i=1}^{N} \xi_i^{\alpha L}(\boldsymbol{x_1}) \xi_i^{\alpha R}(\boldsymbol{x_0}) \, e^{-\lambda_\alpha t} \\ &= \sum_{\alpha \geqslant 1} \sum_{i=1}^{N} \xi_i^{\alpha h}(\boldsymbol{x_1}) \xi_i^{\alpha h}(\boldsymbol{x_0}) \, e^{-\lambda_\alpha t}. \end{aligned} \tag{90}$$

Because H is quadratic in the fermions, the evolution for the $a_i^\dagger$ is linear, and we have in terms of the trajectories:[34,35]

$$I(\boldsymbol{x}_0, \boldsymbol{x}_1) = \left\langle \int D[paths]\, \mathrm{Tr}\mathbf{U}_{path}\ \Pi_l\, \delta[\dot{x}_l + E_{,l} - \eta_l] \right\rangle_\eta$$
$$= \int D[paths]\, \mathrm{Tr}\mathbf{U}_{path}\, e^{-S_{path}}, \tag{91}$$

where the sum is over all paths going from $\boldsymbol{x_1}$ to $\boldsymbol{x_0}$, and the average is over the noise η realization. S_{path} is the usual Langevin action[34]

$$S_{path} = \int_0^t d\tau \frac{1}{4T} \sum_{i=1}^{N} [\dot{z}_i^2 + E_{,i}^2 - 2T E_{,ii}] + \frac{1}{2T}[E(\boldsymbol{x_1}) - E(\boldsymbol{x_0})]. \tag{92}$$

$\mathbf{U}(t)$ is the matrix solution of the linear equation

$$\dot{U}_{ij} = -\sum_{k=1}^{N} E_{,ik} U_{kj} \qquad U(0) = \boldsymbol{I}, \tag{93}$$

which depends on the path through $E_{,ik}$. It describes the linear transformation of a small region around the trajectory, defined by a set of nearby initial conditions *and the same thermal noise*. With these notations, we have:

$$I(\boldsymbol{x_0}, \boldsymbol{x_1}) = \sum_{\alpha \geqslant 1} \sum_{i=1}^{N} \xi_i^{\alpha h}(\boldsymbol{x_1}) \xi_i^{\alpha h}(\boldsymbol{x_0}) e^{-\lambda_\alpha t} = \int D[paths]\, e^{-(S_{path} - L^1_{path})}, \tag{94}$$

where we have defined the (pseudo) Lyapunov exponent (with the time included!), for large t:

$$L^1_{path} = \ln\left[\mathrm{Tr}\mathbf{U}_{path}\right]. \tag{95}$$

The prefix 'pseudo' is a reminder of the fact that actually, true Lyapunov exponents is defined on the basis of the trace of $\mathbf{U}\mathbf{U}^\dagger$. For $\boldsymbol{x_0} = \boldsymbol{x_1}$ our matrix $\mathbf{U}$ is symmetric *on average* $\langle U_{ij} \rangle = \langle U_{ji} \rangle$ (a consequence of detailed balance), but not along a single trajectory. We shall return to this point later. For large t, $L^1_{path} = \ln|\lambda^U_{max}|$ where λ^U_{max} is the eigenvalue of $\mathbf{U}_{path}$

with the largest real part. Note that L^1_{path} can be calculated for long times by considering the path and a nearby path starting from an initial condition close to $\boldsymbol{x_0}$ and evolving with the same noise, just as in the computation of an ordinary Lyapunov exponent, or on the basis of the force required to keep the distance between paths fixed.

Consider the trajectories weighted with the modified action (94). We wish to know the distribution of $\boldsymbol{x}$ at an intermediate time t'. Let us compute the expectation of an arbitrary function $B(\boldsymbol{x})$ at t':

$$\begin{aligned}
&\langle B(t', \boldsymbol{x_0}, \boldsymbol{x_1})\rangle \\
&\quad = I^{-1}(\boldsymbol{x_0}, \boldsymbol{x_1}) \int d^N x \sum_{i=1}^{N} \langle - | \otimes \langle \boldsymbol{x_0} | a_i e^{-(t-t')H} B(\boldsymbol{x}) e^{-t'H} a_i^{\dagger} | \boldsymbol{x_1}\rangle \otimes | - \rangle \\
&\quad = I^{-1}(\boldsymbol{x_0}, \boldsymbol{x_1}) \int d^N x \sum_{\alpha\beta \geqslant 1} \sum_{i=1}^{N} \xi_i^{\alpha L}(\boldsymbol{x_1}) \xi_i^{\alpha R}(\boldsymbol{x_0}) \\
&\qquad \times \langle \boldsymbol{\xi^{\alpha L}} | B(\boldsymbol{x}) | \boldsymbol{\xi^{\beta R}}\rangle e^{-\lambda_\beta (t-t') - \lambda_\alpha t'}.
\end{aligned} \tag{96}$$

Considering t' and $(t - t')$ longer than the microscopic times but much shorter than the passage times one can retain only the contributions 'below the gap':

$$\begin{aligned}
\langle B(t', \boldsymbol{x_0}, \boldsymbol{x_1})\rangle = I^{-1}(\boldsymbol{x_0}, \boldsymbol{x_1}) \int d^N x \sum_{\alpha\beta \geqslant 1} \sum_{i=1}^{N} \xi_i^{\alpha L}(\boldsymbol{x_1}) \xi_i^{\alpha R}(\boldsymbol{x_0}) \\
\times \langle \boldsymbol{\xi^{\alpha L}} | B(\boldsymbol{x}) | \boldsymbol{\xi^{\beta R}}\rangle.
\end{aligned} \tag{97}$$

Now, if $\boldsymbol{x_0}$ and $\boldsymbol{x_1}$ are at the states at the ends of a reaction, the factor

$$\sum_{i=1}^{N} \xi_i^{\alpha L}(\boldsymbol{x_1}) \xi_i^{\alpha R}(\boldsymbol{x_0}) = \sum_{i=1}^{N} \xi_i^{\alpha h}(\boldsymbol{x_1}) \xi_i^{\alpha h}(\boldsymbol{x_0}) e^{-\beta E(\boldsymbol{x_1})}, \tag{98}$$

selects the relevant currents,[36] and we obtain:

$$\begin{aligned}
\langle B(t', \boldsymbol{x_0}, \boldsymbol{x_1})\rangle \sim \int d^N x \, \langle \boldsymbol{\xi^L} | B(\boldsymbol{x}) | \boldsymbol{\xi^R}\rangle &= \int d^N x \, \langle \boldsymbol{\xi^h} | B(\boldsymbol{x}) | \boldsymbol{\xi^h}\rangle \\
&= \int d^N x \, \| \boldsymbol{\xi^h}(\boldsymbol{x}) \|^2 B(\boldsymbol{x}),
\end{aligned} \tag{99}$$

where we have assumed the reaction is given by a single $|\boldsymbol{\xi^R}\rangle$. What we have shown is that long paths sample the barrier $\|\boldsymbol{\xi^h}(\boldsymbol{x})\|$. In other words,

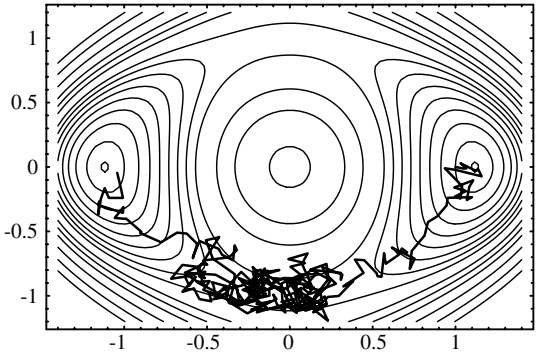

Fig. 8. One typical trajectory with the ends fixed in two different metastable states sampled with Lyapunov+Langevin action. Same potential as in Fig. 7.

trajectories have ends of the order of the microscopic time in $\boldsymbol{x_1}$ and $\boldsymbol{x_0}$, but otherwise spend most of their time in the barrier: see Fig. 8.

If we consider *closed paths* without restrictions on the starting point, we have:

$$\begin{aligned}\int d^N x_0 \, \langle B(t', \boldsymbol{x_0}, \boldsymbol{x_0})\rangle &= \int d^N x_0 \, d^N x \sum_{\alpha\beta \geqslant 1} \sum_{i=1}^{N} \xi_i^{\alpha L}(\boldsymbol{x_o}) \xi_i^{\alpha R}(\boldsymbol{x_0}) \langle \boldsymbol{\xi^{\alpha L}} | B(\boldsymbol{x}) | \boldsymbol{\xi^{\beta R}} \rangle \\ &= \sum_{\alpha\beta \geqslant 1} \int d^N x \, \langle \boldsymbol{\xi^{\alpha L}} | \boldsymbol{\xi^{\beta R}} \rangle \langle \boldsymbol{\xi^{\alpha L}} | B(\boldsymbol{x}) | \boldsymbol{\xi^{\beta R}} \rangle \\ &= \sum_{\alpha \geqslant 1} \sum_{i=1}^{N} \int d^N x \, |\xi_i^{\alpha h}(\boldsymbol{x})|^2 B(\boldsymbol{x}), \end{aligned} \tag{100}$$

where the sums are only over the 'eigenvalues below the gap'; this means that we perform a flat sampling over all barriers: see Fig. 9. If instead of $\|\boldsymbol{\xi^h}(\boldsymbol{x})\|^2$ we wish to sample the squared current $\sum_{i=1}^{N} \xi_i^R \xi_i^R = e^{-\beta E} \|\boldsymbol{\xi^h}(\boldsymbol{x})\|^2$, we have to add a Gibbs weight *at a single time* in the closed path measure.

We can of course fix only one end, and the situation obtained is as in Fig. 10 sampling the escape paths from one metastable state.

7.1. Higher Index Barriers

The procedure outlined above can be generalized in a straightforward way to higher indices. One starts from:

$$I^{(k)}(\boldsymbol{x_0}, \boldsymbol{x_1}) = \sum_{i_1, \ldots, i_k = 1}^{N} \langle \boldsymbol{x_0} | a_{i_1} \ldots a_{i_k} \, e^{-Ht} \, a_{i_1}^{\dagger} \ldots a_{i_k}^{\dagger} | \boldsymbol{x_1} \rangle, \tag{101}$$

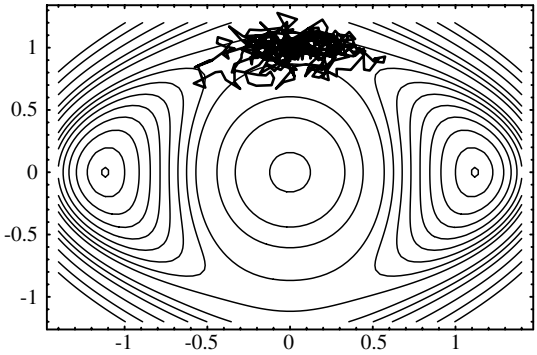

Fig. 9. One typical closed trajectory sampled with Lyapunov+Langevin action. Same potential as in Fig. 7.

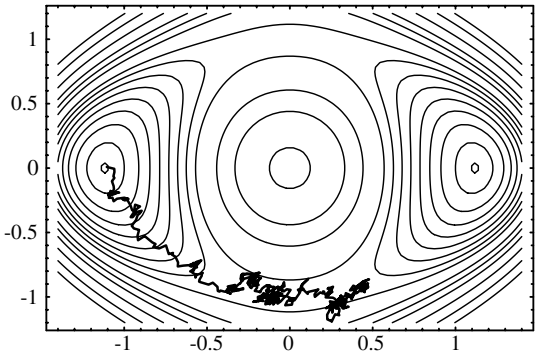

Fig. 10. One typical trajectory with one end fixed in a metastable state and the other left free, sampled with Lyapunov+Langevin action. Same potential as in Fig. 7.

which will select the k-fermion eigenstates 'below the gap'. Again, the evolution of each fermion is linear, and a straightforward calculation[39,35] shows that the path-integral reads:

$$I^{(k)}(\boldsymbol{x_0}, \boldsymbol{x_1}) = \int D[paths] e^{-(S_{path} - L^{(k)}_{path})}, \tag{102}$$

where $L^{(k)}_{path}$ is the (pseudo) Lyapunov exponent, defined as

$$L^{(k)}_{path} = \ln \left[\sum_{i_1,\ldots,i_k=1}^{N} det_p(U, i_1, \ldots, i_k) \right], \tag{103}$$

where $det_p(U, i_1, \ldots, i_k)$ are the k minors of U.

For large t, $L^{(k)}_{path}$ is the sum of the logarithms of the k eigenvalues $\boldsymbol{U}_{path}$ having the largest real parts. $L^{(k)}_{path}$ is a measure of the expansion of k-dimensional surfaces defined by nearby trajectories subjected to the same noise.[35] Just as before, trajectories weighted with $L^{(k)}_{path}$ will pile up in index k barriers.

Before concluding this section, let us point out that, unlike the true Lyapunov exponents defined in terms of $\mathbf{U}^{\dagger}\mathbf{U}$, the ones we are using here are real on average, but there could be rare trajectories for which they are imaginary. The practical procedure is then to separate trajectory space in those that have a real, and those that have imaginary value of $L^{(k)}_{path}$. As usual in these cases, the separation is natural since $L^{(k)}_{path}$ diverges in the frontier.

8. CONCLUSIONS

In this article we have shown how the constructions based on supersymmetry can shed new light on statistical mechanical questions, providing definitions and computational schemes for barriers beyond the low-temperature or the mean-field cases.

We have deliberately avoided maximal generality at each step, in various cases leaving the most general derivations for the Appendices. We have also not attempted full mathematical rigor. The aim has been to convince the reader that all developments are elementary, though we believe quite useful. There are three important omissions:

- Continuous symmetries, leading to non-isolated saddle points and barriers: the subject of degenerate Morse theory.[17] The formalism adapts itself rather naturally to this case, so we are confident that the discussion in this direction can be made more complete.
- Dynamics with inertia (Kramers equation). This is important for practical applications, in which reaction paths have to be found in systems with inertia.

Hamilton's equations do possess a supersymmetry, as shown by Gozzi and Reuter (see ref. 39, and references therein), who used it to rederive some very early results by Ruelle[40] where Hamiltonian, as opposed to Langevin, dynamics is used to study the topology of the space. Part of this supersymmetry survives for the Kramers equation,[41] so the results in this paper, and indeed all the construction related to Morse Theory, can be extended to that case. This is a promising line of research, with a considerable number of applications including, apart from the study of reaction paths, the determination of Ruelle-Pollicott resonances in chaotic systems.

- One can ask if the approach presented in this paper is applicable only to smooth energy functions in space, since there are real problems with energy functions which have singularities: exclusion or Coulomb interactions, hard walls, etc. It is possible to obtain rules for the behavior of particles (or rather, the forms attached to them) after a collision with a hard wall without having to integrate the bounce trajectory every time, by deriving the effect of a regularized wall in the limit of infinite steepness. Using this method it is possible to construct diffusion equations for problems which are entirely entropic, such as hard spheres.
- The question of the application to full quantum evolution remains open. There is of course the less general possibility of coupling the present scheme to a Carr-Parrinello approach, the dynamics being essentially classical in that case.

Work is in progress,[42,41] stimulated by the prejudice that things that are pleasant should also be useful.

APPENDIX A

In his Appendix we sketch the proof that the only zero energy eigenstates of the Hamiltonian (13) is the Gibbs measure (22). The proof will be made using the hermitian basis.

Each eigenstate $|\psi^h\rangle$ of energy zero must be annihilated by both Q and $\bar{Q}$. Indeed, the definition of the zero-energy state:

$$\begin{aligned} 0 &= \langle \psi^h | H^h | \psi^h \rangle \\ &= \langle \psi^h | \frac{1}{T} (\bar{Q}^h + Q^h)^2 | \psi^h \rangle \\ &= \langle \psi^h | \frac{1}{T} (\bar{Q}^{h\dagger} \bar{Q}^h + Q^{h\dagger} Q^h) | \psi^h \rangle \\ &= \frac{1}{T} (\| \bar{Q}^h | \psi^h \rangle \|^2 + \| Q | \psi^h \rangle \|^2), \end{aligned} \tag{A1}$$

is equivalent to

$$Q^h | \psi^h \rangle = 0, \quad \bar{Q}^h | \psi^h \rangle = 0. \tag{A2}$$

Let $|\psi^h\rangle$ be a state with $p > 0$ fermions such that $\bar{Q}^h | \psi^h \rangle = 0$. If we construct the state

$$|\chi^h(y)\rangle = i e^{-\beta E(y)/2} \int_0^1 dt\, t^{p-1} \sum_{i=1}^{N} y_i a_i e^{\beta E(yt)/2} |\psi^h(yt)\rangle, \tag{A3}$$

one can easily verify that

$$\bar{Q}^h|\boldsymbol{\chi}^h\rangle = |\boldsymbol{\psi}^h\rangle. \tag{A4}$$

This in turn means that

$$\langle\boldsymbol{\chi}^h|Q^h|\boldsymbol{\psi}^h\rangle = \langle\boldsymbol{\psi}^h|\bar{Q}^h|\boldsymbol{\chi}^h\rangle = \| \, |\boldsymbol{\psi}^h\rangle \, \|^2 > 0, \tag{A5}$$

which is incompatible with $Q^h|\boldsymbol{\psi}^h\rangle = 0$; we have proved that states with 1 fermion or more cannot be annihilated simultaneously by $\bar{Q}^h$ and Q^h therefore they cannot have zero energy.[43]

On the other hand, if $|\boldsymbol{\psi}^h\rangle$ has no fermions, Eq. (A2) can be written as:

$$\left(T\frac{\partial}{\partial x_i} + \frac{1}{2}E_{,i}\right)\psi^h(\boldsymbol{x}) = 0 \quad \forall i, \tag{A6}$$

and this has only one solution $\psi^h(\boldsymbol{x}) = c_o e^{-\beta E(\boldsymbol{x})/2}$ (22).

Using standard arguments one can show that, for an energy E bounded from below and satisfying Eq. (8), $|\boldsymbol{\chi}^h\rangle$ and $e^{-\beta E/2}$ have a norm, and thus are in the Hilbert space associated with H^h. The conclusion is that the only zero energy state of H^h is

$$|\boldsymbol{\psi}^{0h}\rangle = e^{-\beta E/2} \otimes |->. \tag{A7}$$

APPENDIX B

In this appendix we write the Morse inequalities derived in Section 3 for the trivial topology in a more general context. The number of exact zero energy states, for each fermion sector (let us call them B_p) does not depend on the energy but only on the topology of the space. To see this, suppose that the energy is changed by $E(\mathbf{x}) \to E(\mathbf{x}) + \delta E(\mathbf{x})$. A short computation yields, to first order:

$$\delta H^h = -\frac{1}{2T}\left[\sum_{i=1}^{N}\delta E_{,i}a_i \, , \, \bar{Q}^h\right]_+ + \frac{1}{2T}\left[\sum_{i=1}^{N}\delta E_{,i}a_i^\dagger \, , \, Q^h\right]_+, \tag{B1}$$

and this has zero matrix elements between states with zero eigenvalue, as they are annihilated by the charges. First order perturbation theory tells us then that the eigenvalues stay zero. One can also exclude the possibility of

a non-zero eigenvalue becoming zero, by applying the previous argument to the reverse perturbation.

For R^N, we have shown that the B_p are

$$B_0 = 1, \quad B_1 = 0, \quad \ldots, \quad B_N = 0. \tag{B2}$$

Thus, following the same arguments as in Section 3 one can write generalize the equalities (30) to:

$$\begin{aligned} M_0 &= B_0 + K_1, \\ M_1 &= B_1 + K_1 + K_2, \\ &\vdots \\ M_N &= B_N + K_N. \end{aligned} \tag{B3}$$

where, again, $K_i > 0, \forall i$.

APPENDIX C

The evolution Eq. (6)

$$\frac{d\boldsymbol{\psi}}{dt} = -H\,\boldsymbol{\psi}, \tag{C1}$$

for a vector

$$\boldsymbol{\psi} = \sum_{i_1,\ldots,i_k=1}^{N} \psi_{i_1,\ldots,i_k} a_{i_1}^{\dagger} \ldots a_{i_k}^{\dagger} |-\rangle, \tag{C2}$$

reads, in components (see Eq. (13)):

$$\dot{\psi}_{i_1<\cdots<i_k} = \sum_{\sigma\alpha} (-1)^{n(\sigma,\alpha)}\, E_{\sigma(i_1),\alpha}\; \psi_{\sigma(i_2),\ldots,\alpha,\ldots,\sigma(i_k)}, \tag{C3}$$

where σ denotes all permutations of k indices, and $n(\sigma,\alpha)$ is the sign of the permutation $(i_1, i_2, \ldots, \alpha, \ldots, i_k) \to (\alpha, \sigma(i_1), \sigma(i_2), \ldots, \sigma(i_k))$. The $\psi_{\sigma(i_1),\ldots,\sigma(i_k)}$ are antisymmetric with respect to permutations of indices. Proposing the evolution for functions of $\tilde{F}(\boldsymbol{x}, \boldsymbol{u}, t)$, where $\boldsymbol{u}$ is the set $u_{i_1,\ldots,i_k}$, themselves completely antisymmetric:

$$\frac{d\tilde{F}}{dt} = -\left[H_{FP} - \sum_{i_1,\ldots,i_k=1}^{N} \frac{\partial}{\partial u_{i_1,\ldots,i_k}} \sum_{\sigma,\alpha} (-1)^{n(\sigma,\alpha)} E_{\sigma(i_1),\alpha}\, u_{\sigma(i_2),\ldots,\alpha,\ldots,\sigma(i_k)} \right] \times \tilde{F}(\boldsymbol{x}, \boldsymbol{u}, t), \tag{C4}$$

we can check integrating by parts that $\psi_{i_1,\ldots,i_k}(\boldsymbol{x}) = \int d^N u\, u_{i_1,\ldots,i_k}\, \tilde{F}(\boldsymbol{x}, \boldsymbol{u}, t)$ evolves according to Eq. (C3). This in turn means that $\boldsymbol{x}$ evolves according to the Langevin equation, while

$$\dot{u}_{i_1,\ldots,i_k} = -\sum_{\sigma\alpha} (-1)^{n(\sigma,\alpha)} E_{\sigma(i_1),\alpha}\, u_{\sigma(i_2),\ldots,\alpha,\ldots,\sigma(i_k)}. \tag{C5}$$

We can also write an equation for normalized variables:

$$v_{i_1,\ldots,i_k} = \frac{u_{i_1,\ldots,i_k}}{\sqrt{\sum_{j_1,\ldots,j_k=1}^{N} u^2_{j_1,\ldots,j_k}}}, \tag{C6}$$

such that Eq. (C4) becomes:

$$\begin{aligned} \frac{dF}{dt} = -\Bigg[& H_{FP} - \sum_{i_1,\ldots,i_k=1}^{N} \frac{\partial}{\partial v_{i_1,\ldots,i_k}} \\ & \times \left\{ \sum_{\sigma\alpha} (-1)^{n(\sigma,\alpha)} E_{\sigma(i_1),\alpha}\, v_{\sigma(i_2),\ldots,\alpha,\ldots,\sigma(i_k)} - v_{i_1,\ldots,i_k}\, \mathcal{N}(\boldsymbol{v}) \right\} \\ & + \mathcal{N}(\boldsymbol{v}) \Bigg] F(\boldsymbol{x}, \boldsymbol{v}, t), \end{aligned} \tag{C7}$$

where:

$$\mathcal{N}(\boldsymbol{v}) = \sum_{i_1,\ldots,i_k=1}^{N} v_{i_1,\ldots,i_k} \sum_{\sigma\alpha} (-1)^{n(\sigma,\alpha)} E_{\sigma(i_1),\alpha}\, v_{\sigma(i_2),\ldots,\alpha,\ldots,\sigma(i_k)}. \tag{C8}$$

The particles perform Langevin diffusion, while the equation of motion for the $\boldsymbol{v}$ read:

$$\dot{v}_{i_1,\ldots,i_k} = -\sum_{\sigma\alpha} (-1)^{n(\sigma,\alpha)} E_{\sigma(i_1),\alpha}\, v_{\sigma(i_2),\ldots,\alpha,\ldots,\sigma(i_k)} - v_{i_1,\ldots,i_k}\, \mathcal{N}(\boldsymbol{v}), \tag{C9}$$

thus preserving the normalization (C6). There is also cloning, proportional to $\mathcal{N}(\boldsymbol{v})$.

The equations of motion for $\boldsymbol{v}$ have an interesting interpretation. Consider a point $\boldsymbol{x}$ and a small oriented k-volume element determined by

$$\begin{aligned} \boldsymbol{V}^{\boldsymbol{k}} &\equiv (\boldsymbol{x}+\delta\boldsymbol{x}_{\boldsymbol{1}}) \wedge (\boldsymbol{x}+\delta\boldsymbol{x}_{\boldsymbol{2}}) \wedge \cdots \wedge (\boldsymbol{x}+\delta\boldsymbol{x}_{\boldsymbol{k}}) \\ &= \mathcal{M} \sum_{i_1,\ldots,i_k=1}^{N} v_{i_1,\ldots,i_k} \hat{e}_{i_1} \wedge \cdots \wedge \hat{e}_{i_k}, \end{aligned} \tag{C10}$$

where $\wedge$ is the external (wedge) product and $\hat{e}_1$ are the basis vectors. We have separated the norm $\mathcal{M}$ from the (normalized) 'direction' $\boldsymbol{v}$ of $\boldsymbol{V}^{\boldsymbol{k}}$. It is straightforward to see ref. 35 that Eq. (C9) indeed gives the evolution of $\boldsymbol{v}$ as the points are carried by the drift, and $\mathcal{N}=\dot{\mathcal{M}}$ gives the expansion rate of the norm of $\boldsymbol{V}^k$. This property is at the basis of the use of the present formalism to study Lyapunov exponents.[35]

Now we can outline a proof that the right k-fermion eigenstates 'below the gap' are concentrated on k-dimensional surfaces spanned by the trajectories descending from a saddle of index k. Let us propose that on such surface we have particles whose $\boldsymbol{v}$ at each point is tangential to such a surface (i.e. it can be generated as in Eq. (C10)), and the density of such particles is constant along the surface. Both features are preserved by the evolution. First, as the particles go downhill, their forms change so as to remain tangential: this is because their evolution are precisely based on the linearized equation on the tangential space. Secondly, the cloning rate is exactly opposite to the expansion rate of a small volume advected downhill: as a region expands its population increases and vice-versa. Furthermore, close to the saddle point the surface density expansion rate is $-A_1, \ldots, -A_k$, (A_i the Hessian's eigenvalue) while the cloning rate for a p-form is: $-A_1, \ldots, -A_p$. Because by assumption $A_1 < 0, \ldots, A_k < 0$ and $A_{k+1} > 0, \ldots, A_N > 0$, the cloning is insufficient to maintain a stationary situation unless $p=k$.

ACKNOWLEDGMENTS

We thank A. Oancea for useful discussions.

REFERENCES

1. P. Hänggi, P. Talkner, and M. Borkovec, *Rev. Mod. Phys.* **62**:252 (1990).
2. J. Langer, *Ann. Phys.* **41**:108 (1967).
3. The context here is close to the one in Moro (see ref. 4 and references therein), specialized to the Fokker-Plank operators; for that case Bovier *et al.* [5,6] give the sharpest estimations of times and an extensive presentation of the mathematical literature. The problem of the identification of the metastable states in master equations was discussed

in a series of papers by Gaveau and Schulmann [7–10], and further put in an illuminating mathematical form by Bovier *et al*. in ref. 11. The same kind of ideas is applied in ref. 12 to the study of complex dynamics. See also ref. 13 for an application and a nonrigorous presentation.
4. G. J. Moro, *J. Chem. Phys.* **103**:7514 (1995).
5. A. Bovier, M. Eckhoff, V. Gayrard, and M. Klein, Preprint (2003a).
6. A. Bovier, V. Gayrard, and M. Klein, Preprint (2003b).
7. B. Gaveau and L. Schulman, *J. Math. Phys.* **39**:1517 (1998).
8. B. Gaveau and L. Schulman, *J. Math. Phys.* **37**:3897 (1996a).
9. B. Gaveau and L. S. Schulman, *Phys. Lett. A* **229**:347 (1996b).
10. B. Gaveau, A. Lesne, and L. Schulman, *Phys. Lett. A* **258**:222 (1999).
11. A. Bovier, M. Eckhoff, V. Gayrard, and M. Klein, *Commun. Math. Phys.* **228**:219 (2002).
12. C. Schütte, Preprint SC99-18, ZIB-Berlin (1999).
13. G. Biroli and J. Kurchan, *Phys. Rev. E* **64**:2001 (2001).
14. H. Risken, The Fokker-Plank equation (Springer, 1996).
15. D. J. Wales, Energy Landscapes (Cambridge University Press, 2003).
16. J. Milnor, Morse Theory (Princeton University Press, 1963).
17. E. Witten, *J. Diff. Geom.* **17**:661 (1982).
18. Historically, the mapping between supersymmetric systems and stochastic dynamics has been derived by Nicolai refs. 19–21 and the relation has been further clarified in refs. 22 and 23.
19. H. Nicolai, *Nucl. Phys.* **B176**:419 (1980a).
20. H. Nicolai, *Phys. Lett.* **89B**:341 (1980b).
21. H. Nicolai, *Phys. Lett.* **117B**:408 (1982).
22. G. Parisi and N. Sourlas, *Nucl. Phys.* **B206**:321 (1982).
23. S. Cecotti and L. Girardello, *Ann. Phys. (N.Y.)* **145**:81 (1983).
24. F. Cooper, A. Khare, and U. Sukhatme, *Physics Reports* **251**:267 (1995).
25. Using supersymmetry and induction, one can show, although we shall not need the result here, that the zero eigenvalues stay zero to all orders in T, and only pick up exponentially small corrections.
26. In fact, using nonperturbative WKB analysis (see ref. [17]) one can prove that, the eigenstates "below the gap" have an energy $\exp(-/T + O(1))$ (compared to the eigenstates above the gap which have an energy $O(1)$ in temperature). The best estimates for the energies below the gap are $K\exp(-/T)$ obtained in the zero-fermion sector by Bovier et al. ref. [6]. For a recent, mathematical, review on the spectrum of the Fokker-Planck operator and the "Witten Laplacians" see ref. [27].
27. B. Helffer and F. Nier, preprint 03-25, Université de Rennes (2003b).
28. In the small temperature limit $t_2 \gg t_1$ meaning that, even though the equilibration inside the wells can be fast, the appearance of a steady current is much slower.
29. This is a global comparison of currents. At these times it could still happen that in regions where the current is negligibly small it is not given by the eigenvectors below the gap. If such a detailed approximation is needed, one has to go to longer times.
30. J. Kurchan and L. Laloux, *J. Phys.* A **29**:1929 (1996).
31. The question has been addressed earlier by people looking for Nicolai [19–21] maps for SUSY systems in the K-fermion sector (see for example ref. [32] and references therein).
32. R. Graham, and D. Roekaerts, *Phys. Rev. D* **34**:2312 (1986).
33. See S. Fahy and D. Hamann, *Phys. Rev. B* **43**:765 (1991), for applications of this kind in Diffusion Monte Carlo techniques.
34. J. Zinn-Justin, Quantum Field Theory, and Critical Phenomena (Clarendon Press, 1996).
35. S. Tanase-Nicola and J. Kurchan, *J. Phys. A* **36**:10299 (2003a).

36. We fix the end states in order to force the paths to go from one metastable state to the other. One can do the same thing by using, instead of the Dirac-delta states $|x\rangle$ other functions defining in some way the metastable state, in a manner close to that used in 'Transition Path Sampling' [37,38].
37. C. Dellago, P. G. Bolhuis, F. S. Csajka, and D. Chandler, *J. Chem. Phys.* **108**:1964 (1998).
38. P. G. Bolhuis, D. Chandler, C. Dellago, and P. L. Geissler, Annu. Rev. Phys. Chem. **53**:291 (2002).
39. E. Gozzi and M. Reuter, Chaos, *solitons fractals* **4**:1117 (1994).
40. D. Ruelle, Inventiones Mathematicae **34**:231 (1976).
41. S. Tanase-Nicola and J. Kurchan (in preparation).
42. S. Tanase-Nicola and J. Kurchan, *Phys. Rev. Lett.* **91**:188302 (2003b).
43. We follow here the proof of the Poincaré Lemma, given in R. Abraham, J. E. Marsden, and T. Ratiu, Manifolds, Tensors, Analysis and Applications (Springer-Verlag, 1988), Chapter 6.